THE ASTROPHYSICAL JOURNAL

AN INTERNATIONAL REVIEW OF SPECTROSCOPY AND ASTRONOMICAL PHYSICS

VOLUME 79 MAY 1934 NUMBER 4

A PHOTO-ELECTRIC STUDY OF W URSAE MAJORIS

By C. M. HUFFER

ABSTRACT

The variable star W Ursae Majoris has been observed with the *photo-electric amplifier* on the 15-inch telescope of the Washburn Observatory. The measures of this eighth-magnitude star are of satisfactory *precision*, the probable error of a single normal magnitude being ±0.011 mag.

A new formula representing the photographic and photo-electric minima has been derived, and it is shown that the *period* of revolution of this system is definitely shortening at the present time.

The solution for the *elements* is partly indeterminate, but the variation of light may be explained by the mutual eclipses of two ellipsoidal bodies slightly unequal in size, mass, and brightness, and both darkened at the limb. A combination of spectrographic and photometric results shows that both bodies are smaller than the sun, with densities 2.0 and 3.3 on the solar standard.

The first photo-electric measures of the well-known variable star W Ursae Majoris were made at the Washburn Observatory in April, 1932. These measures of a star as faint as the eighth magnitude were possible with a 15-inch telescope because of the successful application of an FP-54 vacuum tube to the problem of measuring very small photo-electric currents. All observations made in the spring of 1932 were given in a paper by A. E. Whitford,[1] but, as he pointed out at the time, the light-curve of W Ursae Majoris was incomplete, since one maximum was unobservable because of the low altitude of the star. Accordingly, observations were resumed in November, 1932, and the entire curve was obtained with special emphasis on the phases at the two minima and at the unobserved maximum. About half of the measures were taken by Mr. Stebbins, and we both had

[1] *Astrophysical Journal*, **76**, 219–221, 1932.

the advantage of Mr. Whitford's help in keeping the amplifier in working condition.

It was apparent on the first night of observation that the two minima are unequal—a fact which was confirmed by all subsequent

TABLE I

OBSERVED MINIMA OF W URSAE MAJORIS

J.D.	Observer	Method	E	Residuals		
				Schilt (3)*	Huffer(1)*	
					Photographic	Visual
2415947.367	Müller and Kempf	Vis.	$-17712\frac{1}{2}$	-0^d001	.....	-0^d002
6129.193	Baldwin	Vis.	$17167\frac{1}{2}$	− .007	.....	− .010
6414.288	Müller and Kempf	Vis.	16313	− .007	.....	− .009
6516.397	Fauth	Vis.	16007	+ .008	.....	+ .006
7173.822	Parkhurst and Jordan	Vis.	$14036\frac{1}{2}$	− .003	.....	− .004
7668.445	Tickhoff	Pg.	12554	+ .001	-0^d0008	.....
7905.494	Baldwin	Vis.	$11843\frac{1}{2}$	− .001	.....	− .002
8694.378	Kron	Vis.	9479	− .006	.....	− .007
8748.601	Hertzsprung	Pg.	$9316\frac{1}{2}$	.000	+ .0001	.....
8751.604	Horn	Vis.	$9307\frac{1}{2}$	.000	.....	.000
9951.036	Padova	Vis.	$5712\frac{1}{2}$	+ .003	.....	+ .002
2420527.227	Jordan	Pg.	$3985\frac{1}{2}$	.000	+ .0005	.....
0579.1064	Bemporad	Vis.	3830	− .001	.....	− .001
0980.808	Shapley	Pg.	2626	+ .001	+ .0007	.....
1001.494	Van der Bilt	Vis.	2564	+ .001	.....	+ .001
1546.322	Van der Bilt	Vis.	931	− .002	.....	− .002
1670.436	Hertzsprung	Pg.	− 559	− .001	− .0006	.....
2043.445	Hertzsprung	Pg.	+ 559	+ .001	+ .0015	.....
3094.566	Campbell	Vis.	$3709\frac{1}{2}$	− .004	.....	− .002
3164.4679	Schilt	Pg.	3919	+ .001	+ .0025	.....
3659.749	Schilt	Pg.	$5403\frac{1}{2}$	− .002	− .0009	.....
4225.4292	Schilt	Pg.	7099	− .004	− .0024	.....
4282.482	Hellerich	Vis.	7270	− .003	.....	−0.002
4526.5373	Van Gent	Pg.	$8001\frac{1}{2}$	− .003	− .0017	.....
5871.4279	Walter	Pg.	$12032\frac{1}{2}$	− .003	− .0009	.....
6811.7844	Huffer	Pe.	14851	− .002	+ .0012	.....
7103.7157	Huffer	Pe.	15726	−0.002	+0.0008	.....

*The figure in parenthesis refers to the number of the formula.

measures. Also the times of minima did not agree with those predicted by the elements in Prager's catalogue, the error being slightly more than 0.02 of a period, or about ten minutes. It was therefore desirable to derive a new formula which would represent the observed minima more closely.

Table I gives the observed dates of minimum deduced from the photo-electric observations, and other published minima from papers by Schilt,[2] Hellerich,[3] G. Viola,[4] and other scattered sources. The residuals in column 5 are computed from Schilt's formula (3), which closely represents the photographic minima, and those in columns 6 and 7 from our newly derived formula:

$$\left.\begin{aligned} t_1 = \text{J.D. } 2421856.9401 + 0^d.333637665 \cdot E - 0^d.450 \times 10^{-10} \cdot E^2 \\ \pm 0.0004 \pm 0.000000038 \ \pm \ 0.038 \times 10^{-10}, \end{aligned}\right\} \quad (1)$$

which was obtained by a least-squares solution to fit the photographic and photo-electric minima. The probable error of a single

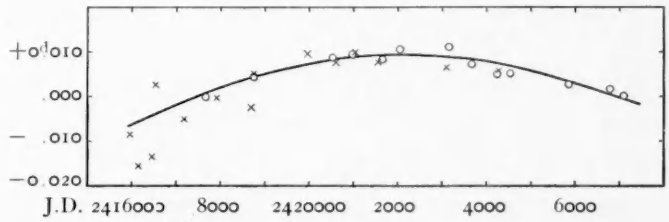

FIG. 1.—Deviation of period of W Ursae Majoris from $P = 0^d.33363758$

photographic or photo-electric minimum is $\pm 0^d.0010$ or $\pm 1^m.46^s$; the probable error of one visual minimum is about three times this amount.

The average period between the first photographic and the final photo-electric minimum is $0^d.33363758$. Figure 1 gives the residuals of all minima in Table I obtained by using this average period. If the period were constant, the residuals should be scattered about zero. This is obviously not the case since the residuals are nearly all positive between the two dates and negative outside. The curve drawn in Figure 1 represents the departure of our new formula from the assumption of a uniform period. This curve satisfies the photographic minima, which are represented by circles; the less accurate visual minima are represented as crosses. The residuals of the ob-

[2] *Bulletin of the Astronomical Institute of the Netherlands*, **2**, 1, 1923.

[3] *Astronomische Nachrichten*, **226**, 127, 1925.

[4] *Rendiconti della R. Accademia Nazionali dei Lincei* (6th ser.), **9**, 743, 1929.

TABLE II

OBSERVATIONS OF W URSAE MAJORIS

Heliocentric Date	Phase	Δ Mag.
J.D. 2426806.6182....	0.517	$0^{M}128$
.6246....	.536	.208
.6315....	.556	.361
.6401....	.582	.471
.6481....	.606	.563
.6575....	.634	.648
.6695....	.670	.668
.6769....	.693	.732
.6847....	.716	.740
.6910....	.735	.727
.7028....	.770	.680
.7140....	.804	.662
.7249....	.836	.652
.7832....	.011	− .040
.7901....	.032	+ .126
.7959....	.049	.199
.8012....	.065	.332
.8082....	.086	.457
.8168....	.112	.509
.8230....	.130	.585
.8289....	.148	.639
.8341....	.164	.814
.8393....	.179	.746
6807.5867....	.419	.411
.5929....	.438	.381
.5985....	.455	.311
.6081....	.484	.101
.6137....	.500	.075
.6199....	.519	.093
.6303....	.550	.285
.6351....	.565	.391
.6397....	.578	.465
.6462....	.598	.578
.6528....	.618	.603
.6603....	.640	.668
.6683....	.664	.667
.6753....	.685	.692
.6815....	.704	.744
.6877....	.722	.770
.6957....	.746	.782
6808.7180....	.810	.717
.7243....	.829	.742
.7312....	.850	.670
.7372....	.868	.572
.7451....	.892	.552
.7506....	.908	.523
.7582....	.931	.260
.7666....	.956	.156
.7749....	.981	.046
.7804....	.997	− .015
.7873....	0.018	+0.003

Heliocentric Date	Phase	Δ Mag.
J.D. 2426808.7936....	0.037	$0^{M}111$
.7999....	.056	.251
.8074....	.078	.437
.8137....	.097	.505
.8220....	.122	.558
.8324....	.153	.692
6810.6474....	.593	.538
.6543....	.614	.525
.6661....	.649	.650
.6827....	.699	.797
.6882....	.716	.762
.6938....	.732	.710
.6987....	.747	.754
.7070....	.772	.732
.7125....	.788	.750
.7180....	.805	.694
.7298....	.840	.675
.7451....	.886	.598
.7506....	.903	.478
.7582....	.925	.326
.7631....	.940	.275
.7686....	.957	.122
.7742....	.973	.067
.7862....	.009	.002
.7928....	.029	.100
.8005....	.052	.258
.8067....	.071	.354
.8143....	.093	.492
.8199....	.110	.558
.8247....	.125	.566
.8296....	.139	.594
6811.5856....	.405	.513
.5974....	.441	.385
.6023....	.455	.248
.6072....	.470	.175
.6127....	.487	.075
.6182....	.503	.105
.6230....	.517	.145
.6300....	.538	.231
.6376....	.561	.378
.6431....	.578	.443
.6473....	.590	.495
6812.6154....	.492	.066
.6224....	.513	.056
.6272....	.527	.136
.6320....	.542	.253
.6362....	.554	.314
.6438....	.577	.426
.6546....	0.609	0.580

TABLE II—*Continued*

Heliocentric Date	Phase	Δ Mag.	Heliocentric Date	Phase	Δ Mag.
J.D. 2426825.7344....	0.813	$0^{M}709$	J.D. 2427041.8158....	0.470	$0^{M}153$
.7406....	.832	.712	.8178....	.476	.151
.7489....	.857	.640	.8198....	.482	.136
.7572....	.882	.610	.8217....	.488	.076
.7656....	.907	.531	.8235....	.493	.068
.7766....	.940	.257	.8254....	.499	.096
.7842....	.962	.112	.8272....	.504	.098
.7911....	.983	.072	.8286....	.508	.135
			.8337....	.524	.167
7036.7263....	.215	.748	.8356....	.529	.181
.7325....	.234	.728	.8374....	.535	.223
.7373....	.248	.734	.8392....	.540	.285
.7428....	.265	.826	.8410....	.545	.279
.7498....	.286	.767	.8428....	.551	.302
.7533....	.296	.812	.8443....	.555	.325
.7583....	.311	.789			
.7622....	.323	.727	7063.6678....	.967	.034
.7692....	.344	.719	.6697....	.972	.037
.7740....	.358	.616	.6742....	.986	.064
.7789....	.373	.601	.6761....	.991	.092
.7844....	.389	.538	.6813....	.007	.064
.7997....	.435	.428	.6831....	.012	.085
.8052....	.452	.344	.6912....	.037	.138
.8108....	.469	.186	.6937....	.044	.198
.8177....	.490	.130	.6987....	.059	.333
.8239....	.508	.043	.7005....	.065	.373
.8287....	.522	.146	.7253....	.139	.603
.8343....	.539	.168	.7266....	.143	.606
.8391....	.553	.365	.7312....	.157	.648
			.7331....	.162	.666
7039.7292....	.216	.802	.7379....	.177	.638
.7417....	.253	.806	.7398....	.182	.709
.7480....	.272	.759			
.7542....	.291	.727	7077.6679....	.929	.400
.7597....	.307	.711	.6699....	.935	.345
.7667....	.328	.699	.6776....	.958	.194
.7743....	.351	.698	.6795....	.964	.133
.7806....	.370	.683	.6844....	.978	.020
.8013....	.432	.441	.6862....	.984	− .031
.8062....	.447	.428	.6925....	.002	+ .008
.8110....	.461	.260	.6944....	.008	− .042
.8165....	.477	.130	.7000....	.025	+ .082
.8221....	.494	.083	.7018....	.030	.048
.8273....	.510	.078	.7070....	.046	.134
.8332....	.528	.140	.7091....	.052	.225
.8408....	.550	.302	.7288....	.111	.534
			.7306....	.117	.521
7041.7801....	.363	.657	.7347....	.129	.534
.7850....	.378	.601	.7365....	.134	.561
.7974....	.415	.496	.7410....	.148	.672
.8023....	.429	.463	.7428....	.153	.683
.8078....	.446	.240	.7492....	.172	.722
.8124....	.460	.233	.7510....	0.178	0.685
.8142....	0.465	0.213			

TABLE II—*Continued*

Heliocentric Date	Phase	Δ Mag.	Heliocentric Date	Phase	Δ Mag.
J.D. 2427103.6007....	0.657	$0^{M}676$	J.D. 2427103.7586....	0.130	$0^{M}603$
.6052....	.670	.686	.7653....	.150	.621
.6097....	.684	.720	.7699....	.164	.683
.6165....	.704	.687			
.6230....	.723	.707	7106.7585....	.121	.632
.6276....	.737	.749	.7635....	.136	.616
.6319....	.750	.733	.7676....	.149	.646
.6366....	.764	.783	.7718....	.161	.676
.6412....	.778	.793	.7760....	.174	.712
.6486....	.800	.756	.7808....	.188	.666
.6549....	.819	.698	.7906....	.218	.792
.6581....	.829	.690	.7947....	.230	.772
.6638....	.846	.695			
.6684....	.860	.655	7116.7770....	.150	.672
.6749....	.879	.540	.7826....	.167	.676
.6820....	.900	.507	.7917....	.194	.704
.6876....	.917	.447	.7976....	.211	.746
.6970....	.945	.241	.8023....	.226	.742
.7031....	.964	.201	.8069....	.239	.769
.7052....	.970	.151	.8199....	.278	.736
.7107....	.986	.053	.8256....	.295	.717
.7125....	.992	.045	.8304....	.310	.667
.7169....	.005	.101	.8350....	.324	.710
.7187....	.010	.071	.8413....	.342	.660
.7244....	.027	.073	.8461....	.357	.647
.7262....	.033	.135	.8581....	.393	.587
.7310....	.047	.175	.8631....	.408	.510
.7331....	.053	.238	.8676....	.421	.487
.7392....	.072	.338	.8719....	.434	.412
.7416....	.079	.373	.8769....	.449	.277
.7472....	.096	.515	.8860....	0.476	0.124
.7531....	0.113	0.593			

served minima from this curve indicate the accuracy of the new formula. If we use the visual minima, rejecting the observation by Fauth (as Hellerich did), the coefficient of E^2 is still larger. We have then definite evidence that the period of W Ursae Majoris is shortening at the present time, but of course the term in E^2 represents only temporarily the amount of the change in period. If this change is due to the motion in an orbit caused by a third body, the period is greater than thirty years and the amplitude of the light-equation is greater than $0^{d}01$, placing the eclipsing system at a distance of one astronomical unit or more from the general center of mass.

It is to be noted that our adopted primary is the deeper minimum, not the primary given in many previous publications. The second-

ary is indicated by the fraction $\frac{1}{2}$ in the epoch in column 4 of Table I. There is some evidence that the secondary comes later than the half-period by about $0^d.0005$, but this has been neglected in the computation.

Table II records the photo-electric observations; the phase is expressed in decimals of the period computed from the preliminary elements,

$$t_1 = \text{J.D. } 2426811.4504 + 0^d.3336357 \cdot E .$$

This period was determined from the minima observed in April, 1932, and in January, 1933, and was used in the solution to fit best

TABLE III

NORMAL MAGNITUDES OF W URSAE MAJORIS

Phase	Difference of Magnitude		Residual	Phase	Difference of Magnitude		Residual
	Normal	Rectified			Normal	Rectified	
$0^P.007$	$0^M.034$	$0^M.376$	$+0^M.001$	$0^P.495$	$0^M.086$	$0^M.428$	$-0^M.003$
.020	.050	.386	− .005	.508	.086	.428	− .007
.036	.126	.447	− .002	.521	.136	.472	+ .003
.065	.330	.609	+ .006	.534	.192	.518	− .003
.088	.463	.697	− .009	.546	.284	.597	+ .021
.114	.558	.736	− .023	.557	.356	.653	+ .039
.128	.568	.716	− .045	.583	.473	.724	+ .013
.142	.622	.740	− .021	.613	.583	.770	+ .010
.152	.660	.758	− .003	.658	.669	.766	+ .005
.165	.706	.780	+ .019	.695	.729	.769	+ .008
.180	.693	.743	− .018	.724	.736	.750	− .011
.213	.756	.766	+ .005	.752	.747	.753	− .008
.245	.772	.766	+ .005	.791	.731	.756	− .005
.286	.753	.762	+ .001	.822	.711	.774	+ .013
.327	.717	.778	+ .017	.848	.664	.772	+ .011
.352	.666	.772	+ .011	.884	.563	.744	− .017
.381	.602	.769	+ .008	.915	.451	.697	+ .002
.416	.480	.722	+ .008	.941	.256	.550	− .031
.438	.381	.664	+ .021	.962	.133	.455	− .005
.453	.307	.614	+ .028	.976	.066	.401	− .001
.468	.185	.511	− .002	0.989	0.035	0.376	±0.000
0.482	0.111	0.448	−0.010				

the observed photo-electric minima. The comparison star a = H.D. 83963, photo-electric magnitude 8.9, was used throughout the measures.

In computing the light-curve, normals were formed in the usual manner by combining six observations into a single normal. The resulting forty-three normals are given in Table III.

The next step was to rectify the curve on the assumption of uniform disks. This was done by Russell's method of plotting l^2 against $\cos^2 \theta$. Since the maxima are unequal, they were equalized by applying a correction of $-0^{M}.006 \sin \theta$ to the normal magnitudes. Then an attempt was made to compute a light-curve to fit the loss of light due to eclipse alone, that is, the rectified curve. This attempt was not successful. It was possible to satisfy one minimum on the basis of uniform disks, but the other minimum could not be made to fit

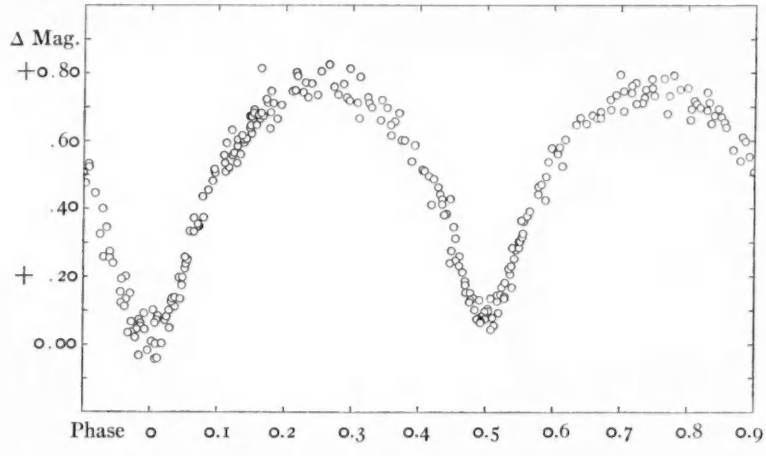

FIG. 2.—Observations of W Ursae Majoris

by any assumption of the value of k. In other words, the two bodies are not uniformly luminous over the disks.

It was then necessary to recompute the correction due to the ellipsoidal shape of the bodies, on the assumption that they are totally darkened at the limb.

The value $Z=0.271$ was obtained by plotting l^2 against $\cos^2 \theta$. Whence

$$z=\epsilon^2 \sin^2 i=0.326 .$$

This assumption of darkened disks with $k=0.75$ gave a satisfactory fit and the elements were computed as given in Table IV. The probable error of a single normal between minima is $\pm 0^{M}.0117$, and during minimum $\pm 0^{M}.0104$.

The larger star is the brighter but has the smaller surface in-

tensity. The difference of magnitude between the components is $0^{M}.46$, which checks with the statement of Adams and Joy[5] that "the spectra of both components appear, the lines of the primary being slightly stronger than those of the secondary."

By using the spectroscopic results of Adams and Joy,[5] the masses and densities may be computed. The only notable changes from their elements are in the densities of the stars. Since in the present solution the more massive star is the larger, its computed density is reduced from 2.8 to 2.0 and the density of the smaller star is in-

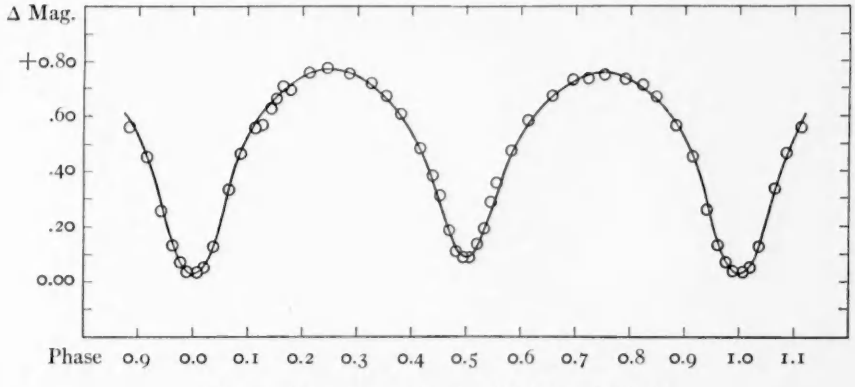

FIG. 3.—Normal magnitudes of W Ursae Majoris

creased from 1.9 to 3.3. The latter density remains, therefore, one of the highest known in any stellar system, except the white dwarfs.

From Eddington's mass-luminosity curve, the visual absolute magnitudes are +5.8 and +6.3, respectively, from which the parallax is $0''.029$, on the assumption that the visual magnitude is 7.9 at maximum. The observed trigonometric parallax is given as $0''.019$ in the Yale catalogue of parallaxes.

In spite of the shallow eclipses (less than $0^{m}.4$ after rectification), which make the solution partly indeterminate, the photo-electric observations point to certain definite results: (1) The period is decreasing at the present time, as is shown by published minima observed over a period of thirty years. (2) The two minima are unequal. This has been suspected by other observers, but the evidence has been somewhat uncertain. (3) The bodies are not equal in size.

[5] *Mount Wilson Contributions*, No. 8, 359, 1919.

(4) The evidence for darkening at the limb is conclusive. (5) The high densities of the components are confirmed.

TABLE IV

ELEMENTS OF W URSAE MAJORIS

Period	P	$0^d.333637665 - 0^d.000 \times 10^{-10} \cdot E$
Primary minimum, J.D. 242+	t_1	6811.7844
Phase of secondary	$t_2 - t_1$	$0^d.1673$
Amount of eclipse, first body	a_0''	.653
Amount of eclipse, second body	a_0	.760
Ratio of radii	k	.75
Loss of light at t_1	$1-\lambda_1$	.300
Loss of light at t_2	$1-\lambda_2$	.264
Light of first body	L_1	.605
Light of second body	L_2	.395
Ratio of surface brightness	J_1/J_2	0.86
Inclination of orbit	i	74°.6
Radii of first body	a_1	0.405
	b_1	.327
	c_1	.275
Radii of second body	a_2	.304
	b_2	.245
	c_2	.206
Ellipticity constant	z	.326
Eccentricity of figure	ϵ	0.59

SPECTROSCOPIC ELEMENTS BY ADAMS AND JOY

Spectrum	.....	F8p
Eccentricity of orbit	e	0
Half-range of velocity	K_1	134 km/sec.
	K_2	188 km/sec.
Minimum mass	$m_1 \sin^3 i$	$0.67\odot$
	$m_2 \sin^3 i$	$.48\odot$
Mass of first body	m_1	.75*
Mass of second body	m_2	.54
Radii of first body	a_1	.89
	b_1	.67
	c_1	.60
Radii of second body	a_2	.72
	b_2	.54
	c_2	0.45
Density of first body	ρ_1	1.96
Density of second body	ρ_2	3.33
Distance between centers	a	1525000 km
Absolute visual magnitude, first body	M_1	+5.8
Absolute visual magnitude, second body	M_2	+6.3
Computed parallax	π	$0''.029$
Observed trigonometric parallax	π_0	$0''.019 \pm 0''.007$

*Sun = 1. This applies to remainder of this column.

It is a pleasure to acknowledge the part of Professor Joel Stebbins and Dr. A. E. Whitford in this study. The latter perfected the amplifier and supervised its operation throughout the measures. The former shared the observations, critically examined the results, and suggested improvements in the preparation of this paper. This work was supported in part by a grant from the National Research Council.

WASHBURN OBSERVATORY
MADISON, WISCONSIN
December 1933

THE VARIABLE SPECTRUM OF VV CEPHEI

By DEAN B. McLAUGHLIN

ABSTRACT

VV Cephei is of spectral class gM2, with wide emission lines of *H* and *Ca* II centrally divided by sharp absorption, and narrow emission lines of *Fe* II, both permitted and forbidden. A faint spectrum of earlier type, possibly B, is present. The *H* and *Ca* II emissions undergo structural changes, the intensity ratio *V*/*R* changing from 0.8 to 4.

During 1932 and 1933 the class M absorption spectrum showed a velocity range of 10 or 12 km/sec., with two maxima and two minima during one light cycle. Principal light maximum occurred near the time the velocity decreased through its mean value of −34 km/sec.

The absorption lines of *H* show a variation of velocity of 30 km/sec. range, correlated with the variation of *V*/*R* as in a Be star. Minimum velocity occurred after principal light maximum, and maximum velocity after light minimum. The mean *H* velocity is positive with respect to the class M spectrum by about 45 km/sec. The H and K lines of *Ca* II may vary with *H*, but they are shifted only +15 km/sec. from the class M spectrum. The narrow *Fe* II emission is stationary, with a shift of +15 km/sec. from the class M spectrum.

The class M star is considered to be pulsating. The phase relations of light and velocity are not unfavorable to this interpretation. The variations of structure of *H* emission and velocity of *H* absorption are interpreted as due to expansion and collapse of a rotating atmosphere of *H* under variable radiation pressure from the star. Phase relations of light and *H* velocity are distinctly favorable to this view. Some systematic shifts of hydrogen emission are explained by partial occultation of the atmosphere by the star. The *Fe* II emission is referred to a nebula enveloping the system.

This star[1] was added to the Ann Arbor spectrographic program in August, 1932, as part of an intensive study of the light-curves and spectra of bright irregular variables. A feature of special interest was the possible affinity with spectra of class Be, indicated by a description of the spectrum by Adams and Joy.[2]

THE LIGHT VARIATIONS

Between June, 1932, and December, 1933, the writer made more than two hundred comparisons of the variable with ξ Cephei and 18 Cephei. The individual observations will be published elsewhere. The observed light-curve is plotted at the top of Figure 1. Primary minima occurred about July 20, 1932, and July 5, 1933, and a broad flat secondary minimum lasted through November and December, 1932. A sharp primary maximum occurred about February 15, 1933, and secondary maxima October 15, 1932, and October 20, 1933. The

[1] HD 208816, R.A. 21^h53^m8, Dec. $+63°9'$, 1900. Spectrum M2ep.

[2] *Publications of the Astronomical Society of the Pacific*, **33**, 263, 1921.

length of the cycle observed is about one year, and a similar trend is recognizable in the spectral changes.

GENERAL DESCRIPTION OF THE SPECTRUM

The absorption spectrum is of class gM2. Upon this are superimposed wide emission lines of hydrogen, $H\beta$ being the strongest in the photographic region. They are divided almost centrally by sharp absorption lines, not often clearly seen at $H\beta$, but always strong and sharp at $H\gamma$, and very strong at all higher lines of the Balmer series, as far as they are observed. Narrow bright lines of *Fe* II, both permitted and forbidden, are very conspicuous; and there are at least two other similar emission lines, λλ 3993 and 4069, the first unidentified and the second tentatively referred to *S* II. H and K of *Ca* II are strong narrow absorption lines with conspicuous emission edges.

Toward the shorter wave-lengths the absorption lines of the class M spectrum become gradually less conspicuous, presenting a "washed-out" appearance, even on strongly exposed plates. The continuous spectrum can be seen extending with very slight, but nearly constant, intensity far into the ultra-violet; on one plate it was certainly seen at λ 3620, but no lines except those of hydrogen have been clearly distinguished at wave-lengths shorter than 3900. On two plates the writer has suspected the presence of λ 3820, *He* I, but coarse-grained underexposed spectra are a fertile field for the cultivation of subjective effects. No abnormality appears at λ 4009 or λ 4026, so that the evidence as to the other spectrum rests solely upon the great extent in the violet. The writer suggests, however, the possible presence of a B-type companion.

MEASUREMENT OF THE SPECTROGRAMS

During approximately sixteen months, eighteen spectrograms of VV Cephei have been taken with the single-prism spectrograph, which has a dispersion of 40 A/mm. at $H\gamma$. Velocities of the class M absorption spectrum are based on a uniform set of 25 lines. The hydrogen emission and absorption, the narrow emission lines, and H and K of *Ca* II were measured twice. The hydrogen emission velocities depend on measures of the outer edges of the emission, but

the narrow emission lines were bisected in the usual manner. The velocities of *Fe* II, permitted, depend on only two lines, λ 4179 and λ 4233, as all others are badly blended with the class M spectrum. Five of the forbidden lines were measured for velocity: λλ 4244, 4277, 4287, 4414, and 4416.

Table I gives the velocities of the several different groups of features and of individual lines of hydrogen and *Ca* II. Velocity-curves of the several features are plotted in Figures 1 and 2, with the light curve and the curve of emission ratio V/R.

STRUCTURAL VARIATIONS OF EMISSION LINES

The hydrogen emission lines are subject to conspicuous changes in the relative intensity of the two components into which they are divided by the absorption. At one extreme the two components are nearly equal, with that of greater wave-length (red component) slightly the stronger. At the other extreme the red components of all lines except $H\beta$ and $H\gamma$ practically vanish and the violet components become greatly intensified, so that the hydrogen spectrum resembles that of P Cygni, with the positions of bright and dark lines interchanged. "Emission ratios V/R" are tabulated in the last column of Table I. These are based upon estimates of the ratio of intensity of violet to red component at $H\gamma$ and $H\delta$. Plate IX shows the changes at $H\gamma$ and $H\delta$.

The emission about the H and K lines shares this variation. As nearly as can be judged, the changes are synchronous with those of the hydrogen lines. The *Ca* II emission is weaker and is not at all conspicuous when the hydrogen components are equal. When the violet hydrogen components are strong, however, the violet *Ca* II components become conspicuous. The red component of the H line cannot be observed, owing to the presence of the violet component of $H\epsilon$.

The curve of emission ratio is plotted in Figure 1 beneath the light-curve and is repeated in Figure 2. The greatest strength of the red component occurred some time after maximum light. The violet component did not begin to strengthen rapidly until near light minimum, and its greatest intensity has lasted long after light minimum. The curve of emission ratio resembles roughly the light-

PLATE IX

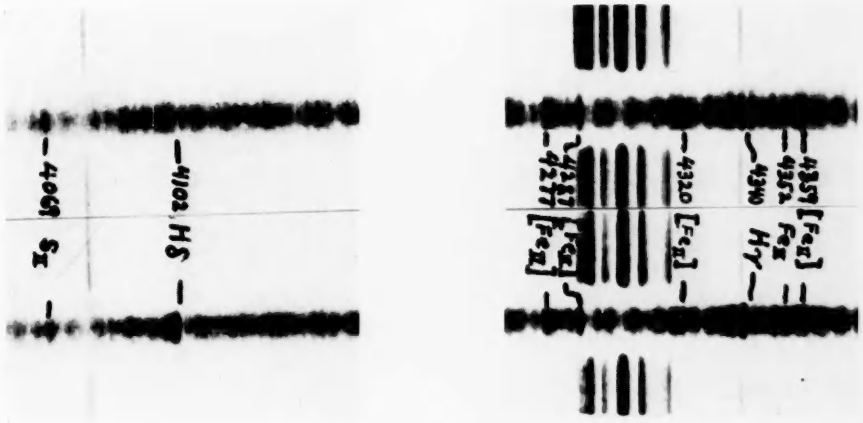

CHANGES OF $H\gamma$ AND $H\delta$ IN THE SPECTRUM OF VV CEPHEI

a) April 27, 1933
b) June 17, 1933

UNIV. OF MICH.

TABLE I

VELOCITIES OF SELECTED FEATURES IN THE SPECTRUM OF VV CEPHEI

Date U.T.	Class M Absorption Velocity (Km/Sec.)	Hydrogen Absorption Velocities				Hydrogen Emission Velocities			Ca II		Sharp Emission		Emission Ratio (V/R)
		$H\gamma$	$H\delta$	$H\epsilon$	$H\zeta$	$H\beta$	$H\gamma$	$H\delta$	H	K	*Fe* II	[*Fe* II]	
1932													
Aug. 9.35	−33	+ 6	+ 4	+16	+ 8	+15	−10	+14	−22	+ 4	−23	−20	2.1
Sept. 29.32	38	+15	+17	+18	+10	−45	−10	− 1	−31	+ 2	16	20	2.8
Nov. 6.19	38	+17	+ 5	+10	+ 2	−27	+ 6	+ 4	−35	− 8	23	17	1.7
Dec. 17.09	29	+12	+ 6	+ 9	− 2	−22	+ 3	+12	−28	−28	16	17	0.85
1933													
Jan. 30.04	30	0	+ 7	+ 9	+ 8	−39	0	+21	−20	−20	14	15	0.9
Mar. 28.42	39	−15	+ 7	.....	.....	−50	− 8	.....	.....	.....	.....	19	1.3
April 27.31	42	− 6	− 3	−12	−12	−58	+ 3	.....	−30	−38	21	24	0.75
May 18.36	33	+ 4	− 6	+12	+ 7	−30	− 9	.....	−27	−23	19	18	0.95
June 4.34	32	+ 8	+ 1	+ 9	0	(−28)	+ 1	− 3	−24	−24	13	16	1.2
June 17.26	32	+10	+ 7	+ 1	− 9	−33	−15	−35	−26	− 7	22	14	3.1
July 1.37	35	+10	+16	.....	.....	−24	− 2	.....	.....	.....	(25)	13	3.0
July 19.36	30	+ 7	+21	+22	+13	−14	+ 8	+11	−10	.....	23	15	2.8
Aug. 2.34	32	+17	+26	+31	+22	−29	− 8	.....	−35	−22	28	20	4
Aug. 11.37	34	+23	+23	+10	+12	−31	− 5	+ 2	−24	−16	26	16	3.0
Sept. 30.20	35	+21	+22	+20	+25	− 1	− 3	+11	−18	(+ 3)	21	18	3.3
Oct. 8.24	36	+ 9	+15	+14	+10	0	+ 4	+ 7	−29	−18	20	20	2.4
Oct. 28.24	31	+18	+24	+35	+ 2	−49	+ 5	.....	(+ 1)	− 4	−28	22	4
Dec. 1.10	−31	+ 5	+16	.....	.....	−10	0	(+ 4)	.....	.....	(−23)	−21	1.6
Means	−33.9	+ 9.0	+11.5	+13.6	+ 6.4	−26.3	− 2.3	+ 3.9	−25.6	−15.5	−21.3	−18.1	

curve inverted and shifted along the time axis in the positive direction about one-quarter of a cycle.

No appreciable changes of relative intensity between line and line or between lines and continuous spectrum have been noted in the narrow emission lines.

THE CLASS M ABSORPTION SPECTRUM

The mean velocity given by the class M spectrum is -33.9 km/sec. for the epoch 1933.4. In the main the fluctuations of velocity shown in Figure 1 are considered real. If regarded as due to

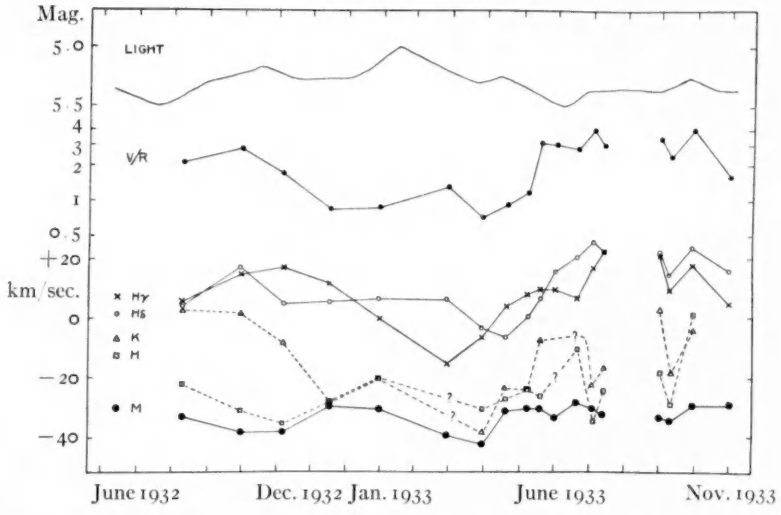

FIG. 1.—Light-curve, V/R variation and absorption velocities of VV Cephei

errors of measurement, the probable error of a single plate would be ± 2.4 km/sec.; whereas experience has shown, for other spectra of class M on plates of similar grain and quality, that the writer's measures of velocity have probable errors of approximately 1.0 km/sec.

Detailed discussion is reserved for a later section, but it is interesting to note that the measures indicate two maxima and two minima of velocity during a cycle of the light variation of the star in which a primary and secondary maximum and minimum occurred. The fact that the primary maximum of light occurred near

the time when the velocity changed from greater than the mean value to less than the mean value is believed to be particularly significant.

THE HYDROGEN LINES

The velocities of the $H\gamma$ and $H\delta$ absorption lines are plotted in Figure 1. They show a range of about 30 km/sec. and a large positive shift with respect to the class M spectrum. The major portion of the variation is unquestionably real, although the reality of the differences shown by the individual lines is questionable. The sharpness of these features is excelled by few lines in stellar spectra. Repetitions of the measures give numerical differences between first and second measures averaging 4 km/sec. for $H\gamma$ and 3 km/sec. for $H\delta$. Dr. A. D. Maxwell has very kindly developed a formula from which the probable errors may be calculated from these differences. The mean of two measures of $H\gamma$ has a probable error of ± 1.7 km/sec., and of $H\delta$, ± 1.3 km/sec.

The correlation between these velocities and the emission ratios is especially striking. The variations of these two quantities follow the course which is typical of spectrum variables of class Be. From the correlation of the light-curve and the curve of V/R it then follows that the hydrogen absorption velocity is related to the light variations of the star. The present case differs from that of a typical Be star in that VV Cephei has not been known to show the red component conspicuously the stronger; whereas in most Be stars the two components share nearly equally. The inequality may be a permanent characteristic of VV Cephei, as Adams and Joy noted it on their spectrograms taken in 1917–1921.

The hydrogen emission velocities are plotted in Figure 2. The changes shown by $H\beta$ are large and apparently systematic, and it appears probable that they are real, so far as their general trend is concerned, even though $H\beta$ is less reliable for velocity measurement than the others. The changes shown by $H\gamma$ and $H\delta$ are smaller than those of the corresponding absorption lines, and do not agree at all with those of $H\beta$. The only surely real systematic changes of $H\gamma$ and $H\delta$ are a sudden negative shift simultaneously with the positive shift of the absorption in June, 1933, and a similar smaller displacement on August 2, 1933. Measures of the edges (not tabulated)

showed clearly that this was due to a flaring-out of the violet emission component. That it was not a photographic effect, however, is plain from the fact that immediately after the sudden change in June the emission edge returned to its normal position, although that component remained at practically the same intensity. Aside from the changes just mentioned, we can consider the hydrogen emission practically stationary during the interval of observation. The pronounced negative shift of the $H\beta$ emission cannot be due to the great intensity of the violet component, for this shift was greatest while

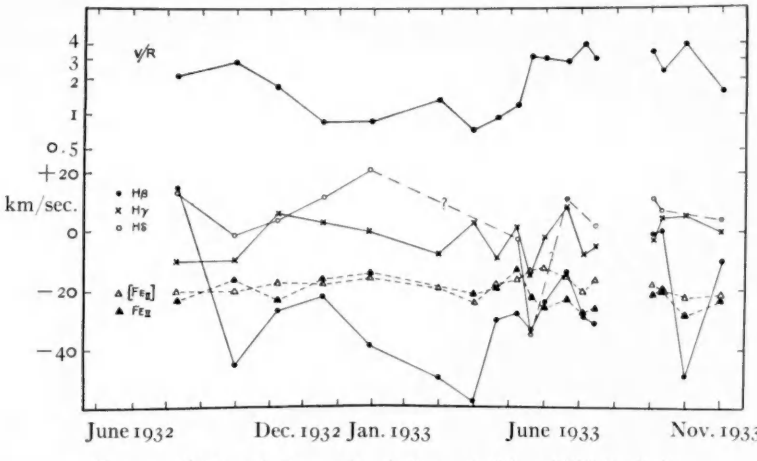

FIG. 2.—V/R variation and emission velocities of VV Cephei

that component was weakest. A suggested interpretation will be given below.

On several plates which show the greatest intensity of the violet emission components a second absorption line with positive displacement has been observed flanking several hydrogen lines. On the plate of June 17, 1933, these were measured at all the lines from $H\epsilon$ to $H\iota$, with an average displacement of +108 km/sec. On a few later plates these lines were measured with displacements of about +150 km/sec. They are not strictly confined to the hydrogen lines, for on the plate of August 2, 1933, such a component was measured beside the K line, with a displacement of +120 km/sec. Whether these are additional absorption lines superimposed on the emission or part of a broad underlying absorption showing up beneath the faded red component cannot now be decided, but the writer favors

the first view. Satellites of hydrogen lines have been observed in several peculiar spectra, notably υ Sagittarii.[3] It is interesting to note a possibly suggestive similarity with the double or multiple absorption lines of novae.

On two plates which showed the ultra-violet region best, all the hydrogen emission and absorption lines which could be seen were measured. On that of June 17, 1933, emission was measured as far out as $H\xi$ and absorption at $H\iota$. On that of August 2 the emission at $H\rho$ was measured, and possible absorption at $H\xi$. Both plates showed the reversed P Cygni character in all the lines. Another plate, taken on April 27, 1933, when the emission components were practically equal, showed the continuous spectrum as far into the violet as those mentioned above, but no emission could be seen beyond $H\zeta$.

The separations of the outer edges of the emission at $H\beta$, $H\gamma$, and $H\delta$ are equivalent to velocities of 377, 322, and 256 km/sec., respectively. This is partly due to the width of slit used, particularly at $H\beta$. The true widths are probably of the order of 200 km/sec. for all the lines.

THE H AND K LINES

The velocities given by H and K of *Ca* II are plotted in Figure 1. Although they show a pronounced negative shift with respect to the hydrogen lines, there is some tendency to accompany those lines in their velocity variations. Some disturbing factor is also at work producing the discrepancy between the velocities of H and K, which is particularly large in the first three plates and recurs, to a smaller extent, in the plates taken after June, 1933. It is tempting to attribute this to the effect of overlapping of the $H\epsilon$ emission on the H line, since the maximum of the effect occurs at the times of great strength of the violet emission components.

To test this, the displacements of the violet edges of the hydrogen and *Ca* II emission were measured on several plates, giving the following mean values:

$H\zeta$	−141 km/sec.	$H\epsilon$	−102 km/sec.
K	−136	$H\delta$	−124
H	−124		

[3] Plaskett, *Publications of the Dominion Astrophysical Observatory*, **4**, 12, 1927.

Obviously, the H and K violet emission edges fall in line with the hydrogen emission at $H\zeta$ and $H\delta$, but the $H\epsilon$ emission edge is clearly cut off by the H absorption. It is therefore concluded that the *Ca* II absorption originates high enough in the stellar atmosphere to be relatively free from superimposed $H\epsilon$ emission.

A possible indication of partial overlap, however, is seen in the behavior of the H line at the time when the violet emission components of $H\gamma$ and $H\delta$ first flared out. The K line, in common with the hydrogen absorption lines, moved in the positive direction, but the H line remained fixed, as if the flaring $H\epsilon$ emission held it back. Later, when the flaring edge had shrunk in, the H line moved in the positive direction, only to move back again when the second flaring of the emission occurred. In this last move, however, it appears to have been accompanied by the K line. On the plate of October 28, 1933, the H line is not clearly distinguishable; in its place is a confused mass of emission.

Since the widths of the emission lines place H and K in a class with the hydrogen lines, it is concluded that they originate in the same general region of the atmosphere as the latter. Possibly, under variable excitation, the effective levels of absorption and emission undergo changes permitting partial overlap of $H\epsilon$ emission on the H absorption.

THE SHARP EMISSION LINES

Many suspected emission features were measured, but most of them were quickly eliminated as merely bits of continuous spectrum between absorption lines. Some other certainly real emission lines are so badly blended with the continuous spectrum that they are of no value for velocity measurement.

The features which are believed to be wholly or partly due to emission, other than the lines of *H* and *Ca* II, are listed in Table II. Discrepancies between the measured and laboratory wave-lengths are discouragingly large in most cases. The seven lines used for emission velocities (two permitted and five forbidden lines of *Fe* II) are indicated by asterisks (*). The average velocity from these lines was assumed to affect all measured emission features, and corrections based upon this assumption have been applied to the tabulated wave-lengths. Lines of *Ti* II and *Cr* II which are associated with

Fe II in the spectrum of η Carinae were searched for but are definitely not present in sufficient intensity to be suspected on the Ann Arbor spectrograms.

The first line, λ 3993, is particularly interesting. To the writer's knowledge it has never been observed before. No line at this position occurs in the nebular spectrum, and there is no conspicuous

TABLE II

WAVE-LENGTHS OF NARROW EMISSION LINES

λ I.A.	Int.	Identification
3993.15	3	Unknown
4068.61	4	4068.62 S II?
4178.87*	5	Assumed *Fe* II
4233.16*	7	Assumed *Fe* II
4243.97*	10	Assumed [*Fe* II]
4276.87*	5	Assumed [*Fe* II]
4287.40*	9	Assumed [*Fe* II]
4296.78	3	4296.56 *Fe* II
4303.59	3	4303.18 *Fe* II
4319.53	4	4319.64 [*Fe* II]
4352.43	3	4351.77 *Fe* II 4352.80 [*Fe* II]
4359.24	4	4358.38 [*Fe* II] 4359.34 [*Fe* II]
4413.79*	5	Assumed [*Fe* II]
4416.28*	5	Assumed [*Fe* II]
4451.74	4	4452.09 [*Fe* II]
4457.70	3	4457.96 [*Fe* II]
4515.38	4	4515.34 *Fe* II
4550.6	4	4549.3 *Fe* II
4556.5	4	4555.9 *Fe* II
4583.54	10	4583.84 *Fe* II
4923.06	4	4923.92 *Fe* II
5017.96	4	5018.44 *Fe* II

* Lines used for velocity.

absorption line at this place in any stellar spectrum. The second line, λ 4069, agrees so closely in position with the line of *S* II in the nebular spectrum that it is tentatively identified with that atom. Other nebular lines were searched for, but no traces of them were found.

The velocities given by the permitted and forbidden lines of *Fe* II are plotted in Figure 2. The scattering of the points is not greater than should be expected for the means of only two and five

lines, respectively, and the velocities are considered constant during the interval of observation. The difference of 3 km/sec. between the means of the two sets is not significant when we consider that several of the lines are undoubtedly influenced somewhat by neighboring portions of the class M spectrum. A possible tendency of the forbidden lines to follow a curve parallel to that of the class M absorption spectrum may be referred to the same cause, or it may be fortuitous. There can be little doubt that the forbidden and permitted lines originate in the same region of the stellar atmosphere.

Many measures of the widths of these emission lines were made. The average of all is in almost precise agreement with the widths of comparison lines of similar intensity. Their true widths are therefore too small to detect with the dispersion and slit-width employed. An upper limit of width should possibly be placed as high as 0.7 A, as a rather wide slit was used in taking the spectrograms.

DISCUSSION

An attempt to interpret the phenomena of this peculiar spectrum must of necessity be highly speculative. Certain correlations between the variable features have been mentioned, and these appear too clear cut to be fortuitous.

Possibly many would consider the evidence of variation of the class M absorption velocity insufficient. The writer does not insist upon the precise values plotted, but after careful consideration of the probable errors of such measures it appears certain that times of maximum and minimum velocity are roughly indicated. The maximum of light occurred approximately midway between maximum and minimum velocity. If we consider the star to be pulsating, maximum velocity corresponds to maximum rate of contraction, and hence the maximum of light occurred when the star was smallest. This is probably the most significant of the correlations which can be pointed out between the variations of light and velocity, and is in good accord with the pulsation hypothesis. The broad, flat minimum of light superimposed upon the rising branch of the light-curve is associated with the largest value of the stellar radius. The correlation of the primary minima is not so good; that of July, 1933, did not occur until the star had begun to collapse again, thus lagging in the same direction as the minimum of a Cepheid variable.

As already noted, the correlation between the hydrogen absorption velocities and the emission ratios is the same as that which is observed in the variable emission lines of Be spectra. It is possible for a binary, such as β Lyrae,[4] to simulate this behavior closely, but in the present case binary motion appears highly improbable. In many Be stars the changes are certainly not due to binary motion, as is attested by the irregularity of their periods. One interpretation, which unfortunately is still current, would ascribe this correlation to a purely photographic effect of crowding of the absorption line by the stronger emission component. Details of the evidence will not be discussed here, but the writer[5] has shown that this interpretation is erroneous as a general explanation, although some minor effects of this sort are not denied.

The relation of emission ratio to velocity finds a simple explanation in the writer's[6] model of a Be star. Briefly, a rotating emitting atmosphere is permitted to expand and contract under the action of gravitation and variable radiation pressure from the star. A consideration of probable velocities and of the effect of Doppler shift upon the possibility of absorption makes it possible to duplicate, qualitatively at least, the observed line contours and velocities. A strong violet emission component corresponds to a contracting atmosphere; a strong red component, to an expanding one. The hydrogen atmosphere of VV Cephei, according to this view, is collapsing most of the time and only expands feebly for a short time. This is rather difficult for the proposed hypothesis unless, at some time, a reversal of the observed structure occurs, or unless the star is enmeshed in a nebula which would be a practically inexhaustible reservoir of hydrogen.

However, we find most other features in good accord with the proposed hypothesis. When the star was faint and outward radiation pressure was at minimum, the atoms of hydrogen were falling in most rapidly. As the star brightened, the rate of infall decreased. As a result of the cumulative effect of outward acceleration, the most rapid rate of expansion did not occur until after light maximum. As

[4] Miss A. C. Maury, *Harvard Annals*, **84**, 230, 1933; Mrs. L. H. McLaughlin, thesis, University of Michigan, 1929, unpublished.

[5] *Publications of the Observatory of the University of Michigan*, **4**, 48, 1931.

[6] *Proceedings of the National Academy of Sciences*, **19**, 44, 1933.

the light faded, the collapse began again; and at the present writing it is still continuing, with somewhat reduced velocity, while the star is slightly brighter than its minimum.

Discrepancies between the velocities of the emission lines are also logically explained by this hypothesis. The pronounced negative shift of $H\beta$ with respect to the other hydrogen lines has been noted. It would be more correct to say that the others are shifted in the positive direction with respect to $H\beta$, and it is predicted that if $H\alpha$ is observed with sufficient dispersion to provide a reliable radial velocity it will be found to agree closely with that of the absorption spectrum. The explanation is to be found in the different effective levels of origin of the several lines. $H\beta$ originates in a greater extent of atmosphere than do any others, except $H\alpha$. Therefore, the portion of the $H\beta$ atmosphere which is occulted by the stellar nucleus is a smaller fraction than for $H\gamma$ or $H\delta$. Since the violet component is partly due to approaching gases on the far side of the star, some of the outer edge of the violet component of each emission line should be occulted, and this fraction would be greatest for the lines originating in the atmosphere of smallest extent. Hence a relative positive shift should affect all emission lines, but $H\alpha$ would be affected least and $H\beta$ next in order.

Differences between the velocities of the several absorption lines of hydrogen, if real, may be attributed to effects of turbulence which should occur in an atmosphere such as that here pictured, and which would produce discrepancies between velocities of lines originating at different effective levels.

The behavior of the H and K lines is the most unsatisfactory aspect of this problem. Their variations of velocity possibly follow those of the hydrogen lines, and their relation to those lines is indicated by the behavior of their emission. Their large systematic difference of velocity, however, sets them apart. Possibly this is due to the advantage which atoms of *Ca* II possess in the utilization of radiation pressure. Having their ultimate lines in the region of relatively strong continuous spectrum, they should be better supported by selective radiation pressure than are the hydrogen atoms whose ultimate lines are in the far ultra-violet and which must rely

for their support upon relatively infrequent absorption while in an excited state.

The emission lines of iron must originate in a totally different region from the hydrogen and *Ca* II lines, for they show no indication of the broadening which affects those lines. In Be stars the *Fe* II emission lines show widths comparable with those of the hydrogen,[7] and in at least one such star they undergo similar structural changes.[8] There is little choice but to place the emitting iron so far from the star that rotational broadening would not be appreciable. Great distance is likewise demanded by the presence of the forbidden lines. Close to the star the mean free time between encounters would be too short to permit the forbidden transitions to occur. An equally great objection is found in the intensity of radiation near the star, the time between absorptions of quanta which would remove the atom from the metastable state being so short that opportunity to emit the forbidden lines would seldom occur.

The precise location of the iron vapor is not so easily decided. If it is part of the atmosphere of the class M star, we should expect it to share the velocity of that star, which it does not. The forbidden lines cannot be absorbed; therefore we cannot explain the difference of velocity in terms of absorption of light from the atoms on the far side by those on the near side of the star. Recession of infalling atoms on the near side and occultation of those on the far side is ruled out by the requirement of great distance. The last remaining possibility appears to be the origin of these lines in a nebula in which the VV Cephei system is enmeshed, and through which the class M star is now approaching the sun in its long-period orbit.

The long-period binary motion of VV Cephei was announced by Christie.[9] A period of about twenty years and a velocity amplitude of about 40 km/sec. are indicated. If we assume the stars to be equally massive, the mass of the system must be of the order of 50 $\odot$, a rather large, but not wholly improbable, value for a pair of which one is a class M giant. With this interpretation the velocity

[7] Struve and Swings, *Astrophysical Journal*, **75**, 169, 1932.

[8] McLaughlin, *Publications of the Observatory, University of Michigan*, **4**, 183, 1932.

[9] *Publications of the Astronomical Society of the Pacific*, **45**, 258, 1933.

given by the iron emission is approximately that of the center of mass of the system, for the present velocity of the class M star is evidently close to the minimum of its velocity-curve, since the Lick velocities[10] show a change from -12.0 to $+4.2$ km/sec. between 1917 and 1921.

The possibility that the emission and absorption lines of hydrogen and *Ca* II belong to the secondary star has been considered, particularly as the amount and direction of the average displacement of the hydrogen absorption lines fit such a hypothesis. But in this event the displacement of the lines of *Ca* II is not so easily explained, and the correlation of light variations with the changes of velocity of the class M spectrum and of the hydrogen lines cannot be accounted for. We may be sure that the light variations observed refer to the class M star, since no changes of intensity of its absorption lines have been noted. If the companion were the variable, its continuous spectrum should almost obliterate many of the class M lines at maximum light.

The secondary star which is tentatively regarded as of type B is the logical source of the excitation of the hydrogen and *Fe* II emission. One is tempted to raise the question whether all long-period variables owe the excitation of their strong hydrogen emission lines to a faint companion of high temperature. Two cases at least (*o* Ceti and R Aquarii) are known in which faint hot stars accompany giant class M variables, and the possible existence of a third is indicated by the present study.

THE OBSERVATORY
UNIVERSITY OF MICHIGAN
December 1933

[10] *Publications of the Lick Observatory*, **16**, 320, 1928.

A STUDY OF THE COLOR INDICES OF 535 FAINT STARS OF KNOWN SPECTRA IN LOW GALACTIC LATITUDES

By EMMA T. R. WILLIAMS

ABSTRACT

The mean colors of 535 tenth- and eleventh-magnitude stars in and near the Milky Way are studied. It is found that close to the galactic plane, tenth-magnitude A stars are 0^M3 more reddened than tenth-magnitude G stars, and this differential reddening increases with increasing magnitude and decreases with increasing distance from the Milky Way.

It is found that the usually quoted values of about 0^M3 per 1000 parsecs for the visual and differential absorption coefficients are not consistent with these data, as is shown in Table V, a photographic absorption coefficient greater than 1 mag. per 1000 parsecs in the galactic plane being indicated for regions within about 700 parsecs of the sun.

MATERIAL

This study is a by-product of the proper motion program of 18,000 stars in 345 selected regions, which is being carried on at the Leander McCormick observatory. Photovisual magnitudes of all the stars and spectra of about 6000 of them have been determined. It is possible to derive color indices by comparing the McCormick photovisual magnitudes with the photographic magnitudes of the *Astrographic Catalogue*, or in some cases with those of the *Henry Draper Extension*, after suitable corrections have been applied for zero point and scale. A comparison of the color indices of stars of known spectra near the Milky Way with those at higher galactic latitudes gives additional information on the problem of absorption of light in the galactic system.

The present investigation has been limited to regions of comparatively low galactic latitude, as is shown in Table I, the region farthest from the galactic plane being at $-25°$. The total number of regions is 35. A greater number was not included on account of the difficulty of securing satisfactory photographic magnitudes, the values in many of the Astrographic zones being too roughly determined to be of use. Furthermore, no region was included which did not contain at least one star of type A fainter than magnitude 9.5. Although color indices of more than 600 stars were determined, about 80 were

not included in the analysis because there were so few other stars in the particular subgroup that the average was not trustworthy.

The regions are fairly representative of the northern Milky Way, some lying in star clouds and some in dark spaces between star clouds.

TABLE I

Galactic Latitude $-6°$ to $+6°$, Averaging $2.°7$			Galactic Latitude $-25°$ to $-9°$ and $+11°$ to $+22°$, Averaging $15.°4$		
Central Star	Galactic		Central Star	Galactic	
	Longitude	Latitude		Longitude	Latitude
31 b Aql	13°	0°	70 Oph	357°	+13°
ζ Aql	13	+5	η Aql	6	−11
γ Aql	14	−6	110 Her	17	+12
α Sge	21	0	β Del	24	−14
δ Sge	22	−2	Cyg 6	48	+18
17 Cyg	35	+5	76 Cyg	55	−10
ε Cyg	42	−5	41 H And	98	−22
γ Cyg	45	+2	α Per	113	− 9
ξ Cyg	52	−3	Lal 6888	120	−13
ε Cep	69	−1	Lal 13427	134	+18
ζ Cep	69	0	47 Aur	134	+14
Pi 1^h159	95	−1	π^3 Ori	158	−25
RT Aur	149	+6	κ Gem	161	+19
1 Gem	153	−2	λ Ori	162	−15
χ′ Ori	154	−5	Lal 15547	166	+22
ε Gem	155	+6	α CMi	179	+11
η Gem	155	−1			
μ Gem	156	+1			
ξ Gem	166	+1			

ZERO-POINT AND SCALE CORRECTIONS

Recently there have been three extended determinations of color indices of stars which agree closely as to the color indices of various spectral classes. Ross and Zug[1] have determined the magnitudes and colors of over 600 Eros comparison stars averaging about ninth magnitude, the average galactic latitude of these stars being about 45°. Seares, Sitterly, and Joyner[2] have found the magnitudes and colors of 359 southern comparison stars for Eros, also averaging about

[1] *Astronomische Nachrichten*, **239**, 289, 1930.

[2] *Astrophysical Journal*, **72**, 311, 1930.

ninth magnitude and at about 40° galactic latitude. Miss Payne[3] has published photovisual magnitudes in the *Harvard Standard Regions* and has derived color indices for about 800 stars of average photovisual magnitude about $8^{M}.5$ and average galactic latitude 35°.

In Figure 1 are plotted the mean color indices as found in each of these three investigations. It is seen that the three agree most satisfactorily except for differences in zero point. The probable reason

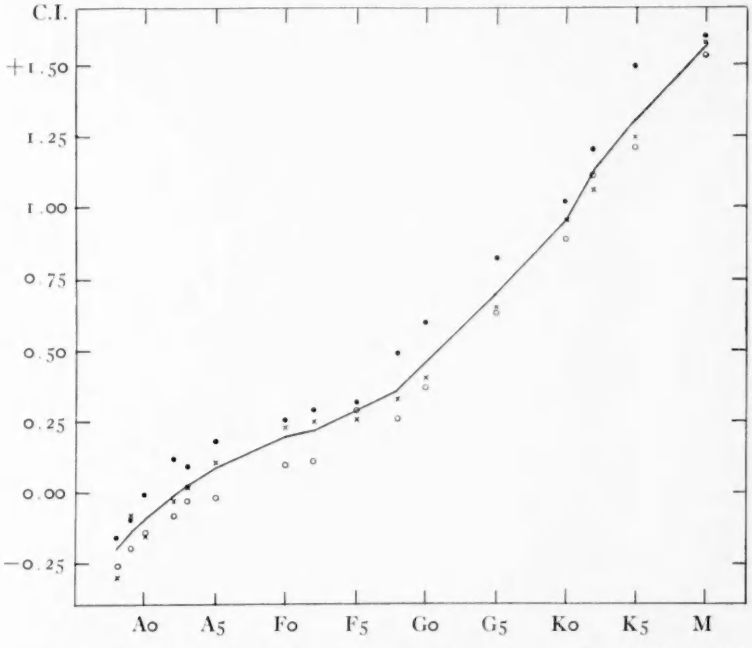

FIG. 1.—The mean color index of each class according to Ross and Zug (crosses); Seares, Sitterly, and Joyner (open circles); and Miss Payne (closed circles).

that Miss Payne's colors are systematically greater than the others is that she found her zero point by assuming that the mean of all the color indices of the stars of spectral class A0 was zero, instead of relying on North Polar Sequence comparisons. However, the precise zero point does not concern us in this paper. A combination of the three sets of color indices gives the values in Table II as "standard" color indices of stars of ninth magnitude well away from the galactic equator.

[3] *Harvard Bulletin*, No. 881, 1931; *Harvard Annals*, **89**, 1, 1931.

In order to find the zero-point and scale corrections of the Astrographic and H.D.E. magnitudes, these standard color indices were added to the photovisual magnitudes of all stars between the spectral classes Fo and K2, thus giving "derived" photographic magnitudes. There were, on the average, ten such stars in each region. The "derived" photographic magnitudes were then compared with the Astrographic or H.D.E. photographic magnitudes, and zero-point and scale corrections for each region were obtained for the Astrographic or H.D.E. magnitudes. In some cases it appeared that there was an appreciable scale error in the McCormick photovisual magnitudes also, in which event suitable corrections were applied. Regions with an insufficient number of stars between Fo and K2 were discarded.

TABLE II

Spectral class	B8	B9	Ao	A2	A3	A5	Fo	F2
"Standard" color index	−.20	−.14	−.09	−.01	+.03	+.09	+.20	+.22
Spectral class	F5	F8	Go	G5	Ko	K2	K5	M
"Standard" color index	+.29	+.36	+.46	+.70	+.95	+1.12	+1.31	+1.57

This procedure assumes that the stars between Fo and K2, in general, are relatively little affected by space reddening, i.e., that they are largely dwarfs and hence at small distances. It would be more desirable to use only G stars for the determination of scale and zero-point errors, since they are so preponderantly dwarfs, but, unfortunately, not enough of them were available. It is believed that on the average the zero-point and scale errors should be fairly well eliminated by this procedure.

RESULTS

The results are summarized in Table III, in the first section of which are listed the observed mean color indices, together with the probable errors calculated from the dispersion of the individual color indices. The more reliable means are printed in boldface type. The number of stars in each of the subgroups is given in italics. The mean color index of all stars in each of the groups F, G, K, and M is given in the last line of the first section for comparison with the "standard" mean color indices tabulated at the bottom. It is seen that the corrections for zero point have been satisfactory, but there is some indication that a slight scale error remains in either the *pv*

TABLE III

Mean Galactic Latitude	Photovisual Magnitude Interval	Bo–B5	B8–A3	A5–F2	F5–Go	G5–K2	K5–M
	Observed Mean Color Index						
2°.7	$9^{M}.51$–$10^{M}.50$	+.37±.03 *10*	+.23±.02 *47*	+.26±.04 *23*	+.44±.02 *41*	+.91±.03 *25*	+1.44±.05 *14*
	10.51–11.50	+.21±.03 *7*	.21 .03 *49*	.30 .07 *11*	.35 .03 *35*	.88 .06 *22*	.....
15.4	9.51–10.50	.....	.22 .07 *13*	.36 .05 *10*	.49 .03 *25*	.98 .04 *39*	+1.36±.04 *19*
	10.51–11.50	.....	.05 .05 *26*	+.40±.04 *9*	.48 .03 *43*	+.87±.03 *43*	.....
	11.51–12.00	.....	.08 .07 *12*	.....	.43 .06 *12*	.....	.....
	9.51–12.00	.....	+.10±.03 *51*	.....	+.48±.02 *80*	.....	.....
All	.....	.....	.....	+.31	+.44	+.91	+1.39
	Standard Mean Color Index						
40	9	.....	−.08	+.17	+.42	+.94	+1.42

or the *pg* magnitudes; this is seen by the fact that in the case of the G and K stars the mean color indices tend to be larger in the brighter groups than in the fainter groups. There may also be a slight color equation in the photographic magnitudes. However, since we propose to compare the color indices of the A stars with those of the G stars in the same magnitude group, these slight errors will be minimized; for, as is seen from the table, the A stars are so much reddened that their color indices differ only two- or three-tenths of a magnitude from those of the G stars. It seems scarcely likely that the photographic magnitudes are affected by a color equation as large as $0^{M}.2$ per magnitude of color index. For if we assume this value of the color coefficient, the color excess of the M stars relative to the G stars will be as large as that of the A stars in the low-latitude group, indicating that the average M star is as far off as the average A star.

It should be mentioned in passing that, within the limits of accuracy of this material, it is impossible to detect the same dependence of reddening on galactic longitude which Zug finds in his material.[4] He has derived values of the color excess in twenty-three galactic clusters and finds that the color excess is greatest at galactic longitude $27° \pm 13°$ and decreases gradually to a minimum at 207°. On the other hand, Becker finds from his observations of the colors of B stars[5] that the stars at longitude 30° are not very greatly reddened—in fact, he has marked a zone between 40° and 60° which seems to be less subject to reddening than most galactic regions, whereas he has found many reddened stars between longitudes 160° and 180°. Again, Stebbins and Huffer,[6] although they suspect a dependence on galactic longitude, find a minimum at longitude 30° and another minimum at longitude 170°. Evidently, the reddening matter is distributed very unevenly, so that generalization is impossible with our present limited knowledge.

DISCUSSION

It is futile to attempt to derive an accurate value of the differential absorption coefficient giving the amount of reddening per 1000

[4] *Lick Observatory Bulletin*, **16**, 119, 1933.

[5] *Zeitschrift für Astrophysik*, **5**, 101, 1932.

[6] *Proceedings of the National Academy of Sciences*, **19**, 597, 1933.

parsecs in the galactic plane (which we shall designate as Δ), when our knowledge concerning the value of the absorption coefficient in visual light (V) or that in photographic light ($V+\Delta$) is so unsatisfactory. Van de Kamp[7] has discussed this difficulty, reviewing the discordant values of the photographic absorption coefficient obtained by Schalén, Trumpler, Bok, and Bottlinger and Schneller, and introducing further evidence on the subject himself. Furthermore, the value derived for Δ also depends on our assumption concerning the effective thickness of the absorbing layer in parsecs (T).

There is now additional evidence in the recently accumulated data on the optical thickness of the galactic absorbing layer in photographic light, herein designated as $T\times(V+\Delta)/1000$, obtained by van de Kamp[7] and by Hubble;[8] also in visual light ($T\times V/1000$) by Carpenter[9] and by Dufay;[10] and, finally, the data on the differential absorption of the galactic absorbing layer ($T\times\Delta/1000$) by Stebbins[11] and by Vyssotsky and Williams.[12] This evidence affords an indirect approach to the problem.

Hubble, from his extensive survey of extra-galactic nebulae, comes to the conclusion that, in photographic light, "the optical thickness of the obscuring medium from pole to pole is 0.5 mag. with an estimated uncertainty of the order of 0.1 mag." This figure excludes the effect of the Barnard obscuring clouds. Van de Kamp's value of $0^{M}8\pm0.2$ includes the effect of the Barnard clouds. In order to exclude the effect of the clouds, Hubble followed two methods: (1) he excluded all regions in which such clouds were even suspected; (2) he included all observed regions except those in which no nebulae at all were found. Hubble points out that in method 1, the effects of selection will give a value smaller than the true optical thickness, whereas in method 2, the effects of selection will give a value larger than the true optical thickness. But we desire a value for the optical thickness in photographic light, with which we may compare the values of the

[7] *Astronomical Journal*, **42**, 97, 1932.

[8] *Astrophysical Journal*, **79**, 8, 1934.

[9] *Publications of the Astronomical Society of the Pacific*, **45**, 227, 1933.

[10] *Publications de l'Observatoire de Lyon* (1st ser.), **1**, fasc. 5, 1933.

[11] *Proceedings of the National Academy of Sciences*, **19**, 222, 1933.

[12] *Astrophysical Journal*, **77**, 301, 1933.

differential absorption of the absorbing layer found from the colors of the globular clusters as measured by Stebbins and by Vyssotsky and Williams. As Hubble states, many of these globular clusters actually lie within the zone of avoidance, so that it will be fair to compare the differential absorption value with the value obtained by Hubble's method 2. In using the material of method 2, we reject the group of observations of galactic latitudes 0°–7° and include in the group from 28° to 37° the fifteen regions mentioned on page 48, and find from a weighted least-squares solution the value $0^{M}.61 \pm .015$ for $T \times (V+\Delta)/1000$, the optical thickness, which may be fairly compared with the results from globular cluster colors and with those from the colors of faint stars obtained in this paper.[13] Parenthetically, if we had used Hubble's values obtained by method 1 and rejected the group of latitudes 0°–7°, we should have obtained $0^{M}.49 \pm .01$.

Stebbins found from his measures of the colors of 45 globular clusters that $T \times \Delta/1000$, the differential absorption experienced by light passing perpendicularly through the Milky Way, is $0^{M}.18 \pm .01$. However, this is based on the assumption that the difference between the color of an Ao star and that of a Ko star is $1^{M}.48$. Since his comparison stars were, on the average, probably fainter than the sixth magnitude, it is probable that this difference is more like $1^{M}.04$ (see Table II),[14] which would reduce his value to $0^{M}.13 \pm .01$. This is confirmed by the work of Vyssotsky and Williams. Although they observed the colors of only 15 globular clusters, their method gives

[13] The group from 0° to 7° has been rejected because the frequency distribution of the 14 observed values of log N is so markedly skew, thus:

Value of log N.....	.26–.50	.51–.75	.76–1.00	1.01–1.25	1.26–1.50	1.51–1.75
Number of regions ..	4	3	3	2	1	1

But the lower limit of the values of log N corresponding to one nebula observed on the plate is about .25, on account of the corrections which Hubble applied to express everything in terms of a one-hour exposure at the zenith. It is obvious from the frequency distribution that this lower limit artificially limits the number of regions and hence *makes the average value of log N too high*. Again, using the value of the optical thickness, $0^{M}.61$, derived from the rest of the data, we find that the expected average value of log N at 5°.1 latitude is +.10, which is lower than the lower limit of about .25. It follows from the Gaussian curve in Hubble's Fig. 8 that the group contains perhaps one-quarter of the true number of regions. If the point corresponding to this group had been included, the value of the optical thickness would have been $0.48 \pm .03$.

[14] For a fuller discussion of this point see *Astrophysical Journal*, **77**, 306–307, 1933.

colors which are probably closer to the I.A.U. system. They find for $T\times\Delta$ the value $0^{M}.11 \pm .02$.

As a general check we may examine the values of $T\times V/1000$. For this we have Carpenter's analysis of the surface brightnesses of extra-galactic nebulae in visual light, in which he used the Holetschek-Hopmann magnitudes and Hubble's classification. By fitting into the usual cosecant relation the points in his figure, which includes practically all of his data (upper left section of his Fig. 1), we find

$$T\times\frac{V}{1000}=+0^{M}.56\pm .14\,.$$

This is to be combined with the value derived by Dufay from the Wirtz measures of surface brightness of the extra-galactic nebulae:

$$T\times\frac{V}{1000}=+0^{M}.14\pm .15\,.$$

Combining these discordant values, we have:

$$T\times\frac{V}{1000}=+0^{M}.35\pm .14\,.$$

This serves as a rough check on the other values, which we give here for comparison:

$$T\times\frac{\Delta}{1000}=+0^{M}.13\pm .03\,,$$

and

$$T\times\frac{V+\Delta}{1000}=+0^{M}.61\pm .05\,.$$

It will be noted that the probable errors assigned to the last two items are three times the formal probable errors. It is quite evident that differential absorption, Δ, must be considerably less than the general absorption, V; probably Δ is not more than half as great as V. Hubble has come to a similar conclusion.

An added complication arises from our ignorance of the way in which the diffuse matter thins out at increasing distances from the

galactic plane. A thin layer, of thickness T and of uniform density throughout, which stops abruptly at a distance $T/2$ from the galactic plane, is frequently assumed, with values of T ranging from 175 to 540 parsecs. Perhaps it is better to assume that the law of thinning out is similar to the approximate law found for stars,[15] namely, that the density is

$$\rho \propto \rho_0^{-2Z/T},$$

where ρ_0 is the density in the galactic plane and Z is the distance from the galactic plane expressed in parsecs. In this case the parameter, T, may be denoted as the "effective" thickness of the layer, since the total diffuse matter in a column of unit cross-section passing perpendicularly through the Milky Way is equal to

$$2\int_0^\infty \rho_0 e^{-2Z/T} dT = \rho_0 T .$$

In the case of A stars the parameter, T, is approximately 200.[16] In the case of later types it is considerably more.[17] From Oort's discussion of all stars taken together, we find that T is 460. By analogy with extra-galactic nebulae turned "edge on," we might expect that the diffuse dark matter thins out more rapidly than the stars in general, so that the value of T for the diffuse matter would be less than 460.

To find how much our interpretation of observations is influenced by our assumptions regarding these factors, we have computed the excess of reddening to be expected in A stars over that found in G stars of the same magnitude, assuming various values of T, V, and Δ. The mean absolute magnitude of the A stars is taken as $+0^{M}5$, and that of the G stars as $+4^{M}0$. The figures resulting from the computations are given in Table IV.

[15] Lindblad, *Meddelanden från Astronomiske Observatorium, Upsala*, **14**, 1926; Petersson, *ibid.*, **29**, 1927; Oort, *Bulletin of the Astronomical Institutes of the Netherlands*, **6**, 249, 1932.

[16] From the work of Lindblad and Petersson, T is about 160 for A stars (see Fig. 2 in Oort's paper); from Becker's spectral *Durchmusterung* (summarized in *Sitzungsberichte der Preuss. Akad. d. Wissenschaften phys.-math. Klasse*, **11**, 1932) a value of about 250 may be derived.

[17] See also in this connection Bottlinger, *Veröff. d. Univ. Sternwarte zu Berlin-Babelsberg*, **10**, No. 2, 1933.

For example, suppose that the effective thickness, T, is 200 parsecs, that V is $1^{M}.0$ per 1000 parsecs in the galactic plane, and that Δ is $0^{M}.5$ per 1000 parsecs in the galactic plane. Then the amount of photovisual absorption (expressed in magnitudes) which is experienced by light coming 900 parsecs from galactic latitude $2^{\circ}.7$ will be equal to

$$\frac{1.0}{1000}\int_{0}^{900} e^{-\frac{r \sin 2^{\circ}.7}{100}}\, dr = 0^{M}.73 .$$

Therefore, the apparent magnitude of an A star of absolute magnitude $+0^{M}.5$ at a distance of 900 parsecs will be

$$m = 0.5 - 5.0 + 5 \log 900 + 0.73 ,$$
$$= 11^{M}.0 ,$$

and the reddening of this star will amount to

$$\frac{0.5}{1000}\int_{0}^{900} e^{-\frac{r \sin 2^{\circ}.7}{100}}\, dr = 0^{M}.37 .$$

Similarly, we find that a G star of apparent magnitude 11.0 at latitude $2^{\circ}.7$ will be 228 parsecs distant, and the reddening will amount to $0^{M}.11$, so that the excess of reddening in A stars over that in G stars of eleventh magnitude at latitude $2^{\circ}.7$ will be $0^{M}.26$, the value which is given in Table IV.

The observed values, to be compared with the computed ones

TABLE IV

EXCESS OF SPACE-REDDENING IN A STARS OVER THAT IN G STARS

Δ	Gal. Lat.	App. Mag.	$T=100$					200					400			
			$V=0^{M}.0$	$0^{M}.5$	$1^{M}.0$	$2^{M}.0$	$3^{M}.0$	$0^{M}.0$	$0^{M}.5$	$1^{M}.0$	$2^{M}.0$	$3^{M}.0$	$0^{M}.0$	$0^{M}.5$	$1^{M}.0$	$2^{M}.0$
$0^{M}.3$	$2^{\circ}.7$	10.1	$0^{M}.13$	$0^{M}.11$	$0^{M}.10$	$0^{M}.09$	$0^{M}.08$	$0^{M}.16$	$0^{M}.14$	$0^{M}.12$	$0^{M}.10$	$0^{M}.08$	$0^{M}.18$	$0^{M}.15$	$0^{M}.13$	$0^{M}.11$
	2.7	11.0	.15	.14	.13	.11	.09	.22	.18	.15	.12	.10	.26	.20	.17	.13
	15.4	11.0	.02	.02	.02	.02	.02	.05	.05	.05	.05	.05	.12	.11	.10	.09
0.5	2.7	10.1	.21	.19	.17	.15	.13	.26	.23	.20	.17	.14	.30	.25	.22	.18
	2.7	11.0	.26	.23	.21	.18	.15	.36	.30	.26	.21	.17	.43	.34	.28	.22
	15.4	11.0	.03	.03	.03	.03	.03	.09	.09	.09	.09	.09	.20	.19	.18	.15
1.0	2.7	10.1	.42	.38	.35	.30	.26	.52	.46	.40	.33	.28	.59	.50	.43	.35
	2.7	11.0	.52	.47	.42	.35	.31	.72	.60	.52	.41	.34	.86	.68	.57	.44
	15.4	11.0	0.05	0.05	0.06	0.06	0.06	0.18	0.18	0.18	0.18	0.18	0.40	0.38	0.35	0.31

given in Table IV, are found as follows: From the first line of the first section of Table III we see that the difference in color between G and A stars is $+0^{M}.21 \pm .03$. Allowing for a color equation of $0^{M}.1$ per magnitude of color index, this becomes $+0^{M}.23$, whereas the "standard" difference is $+0^{M}.50$, with a probable error of about .02. Hence, these A stars of average magnitude 10.1 and galactic latitude $2^{\circ}.7$ are $0^{M}.27 \pm .04$ more reddened than the G stars of the same group, assuming that the differential reddening of the "standard" stars is negligible. But, if $T = 200$, ninth-magnitude A stars at latitude 40° ("standard" A stars) will lie outside the absorbing layer so that they will be reddened as much as the globular clusters at this latitude, whereas the "standard" G stars, being so much nearer, will be only half as much reddened and the "standard" difference of $+0^{M}.50$ quoted above should be increased by $0^{M}.05$ in order to obtain the "normal" difference in color index between A and G stars. This correction happens to have the same value also if $T = 400$, so that in either case the A stars of magnitude 10.1 and galactic latitude $2^{\circ}.7$ are $0^{M}.32$ more reddened than the G stars of the same group; an allowance of $\pm .05$ as probable error is rather liberal. Similarly, the A stars of average magnitude 11.0 and galactic latitude $2^{\circ}.7$ are $0^{M}.40 \pm .05$ more reddened than the G stars of the same group. Again, from the next to the last line of the first section of Table III we find that the A stars of average magnitude 11.0 and galactic latitude $15^{\circ}.4$ are $0^{M}.13 \pm .06$ more reddened than the G stars of the same group. If $T = 100$, the above-mentioned correction is $0^{M}.03$ instead of $0^{M}.05$.

We now have three unknowns, T, V, and Δ, and five observational equations. Denoting the values given in Table IV as $F(T, V, \Delta)$, the equations are

(1) $F(T,V,\Delta)_{m=10.1,b=2^{\circ}.7} = 0^{M}.32 \pm .05$
(2) $F(T,V,\Delta)_{m=11.0,b=2^{\circ}.7} = .40 \pm .05$
(3) $F(T,V,\Delta)_{m=11.0,b=15^{\circ}.4} = .13 \pm .06$

(Values derived above from Table III)

(4) $T \times \dfrac{\Delta}{1000} = .13 \pm .03$ (Stebbins; Vyssotsky and Williams)

(5) $T \times \dfrac{V+\Delta}{1000} = 0.61 \pm .05$ (Hubble's data)

We may now see what values of T, V, and Δ are compatible with the observation equations. In Table V the computed values of the left-hand members of these equations, corresponding to various values of the unknowns, are given for comparison with the observed values. In column 2, for instance, where $T = 200$, $V = 0^{M}.3$, and $\Delta = 0^{M}.3$, all of the computed quantities are much too small, items 1, 2, and 5 all differing from the corresponding observed quantities by

TABLE V

Equation No.	Computed Values							Observed Values
	$T=200$ $V=0^{M}.3$ $\Delta=0.3$	200 $0^{M}.6$ 0.6	400 $0^{M}.3$ 0.3	400 $0^{M}.8$ 0.5	200 $2^{M}.0$ 0.8	160 $2^{M}.5$ 1.0	100 $4^{M}.0$ 1.4	
(1)	$0^{M}.15$	$0^{M}.27$	$0^{M}.16$	$0^{M}.23$	$0^{M}.27$	$0^{M}.29$	$0^{M}.33$	$0^{M}.32 \pm .05$
(2)	.20	.35	.22	.30	.33	.36	.39	.40 .05
(3)	.05	.11	.11	.18	.14	.13	.08	.13 .06
(4)	.06	.12	.12	.20	.16	.16	.14	.13 .03
(5)	0.12	0.24	0.24	0.52	0.56	0.54	0.54	$0.61 \pm .05$

T = effective thickness of absorbing layer in parsecs.

V = visual absorption coefficient per 1000 parsecs.

Δ = differential absorption coefficient per 1000 parsecs.

Observation (1) is the difference in color excess between A and G stars of mag. 10.1 and gal. lat. $2^{\circ}.7$.

Observation (2) is the difference in color excess between A and G stars of mag. 11.0 and gal. lat. $2^{\circ}.7$.

Observation (3) is the difference in color excess between A and G stars of mag. 11.0 and gal. lat. $15^{\circ}.4$.

Observation (4) is the difference between the optical thickness of the galactic absorbing layer in photographic light and that in photovisual light.

Observation (5) is the optical thickness of the galactic absorbing layer in photographic light.

more than three times their probable errors. Hence this combination of values for the unknowns is excluded. Indeed, if the value of T is assumed as 200 parsecs, very much larger values of V and Δ must be taken to satisfy the observations; even assuming, as in the third column, that $V = 0^{M}.6$ and $\Delta = 0^{M}.6$, all of the computed quantities remain smaller than the observed quantities. Of course, if T has been taken too small, the resulting values of V and Δ will be too large. However, even with $T = 400$ parsecs we see from column 4 that it is

impossible to deduce the values $V = 0^{M}3$ and $\Delta = 0^{M}3$, which are so frequently quoted, since items 1, 2, and 5 differ from their corresponding observed quantities by more than three times their probable errors, and all of the computed quantities are smaller than the observed quantities. It is probably significant that it is impossible to obtain such a good "fit" between observed and computed quantities when $T = 400$ as when $T = 200$. Thus, in columns 5–8, values of V and Δ are chosen so as to give the best possible fit corresponding to the given value of T, yet in column 5 the agreement with observation is far from satisfactory. The fit in column 6 may be regarded as satisfactory, but it is perhaps of interest to note that a somewhat better fit may be obtained by assuming the extreme values, $T = 160$, $V = 2.5$, and $\Delta = 1.0$, as in column 7, or $T = 100$, $V = 4.0$, and $\Delta = 1.4$, as in column 8. In this last case, if $T = 100$, then the "observed values" of items 1, 2, and 3 should be decreased by .02, as is explained on page 406. Summing up, although the problem is as yet indeterminate, Table V forces us to the conclusion that the photographic absorption coefficient $(V + \Delta)$ is greater than 1 mag. per 1000 parsecs in the galactic plane. This conclusion applies, of course, only to regions within a distance from the sun corresponding to the distance of the eleventh-magnitude A stars, which is, perhaps, 700 or 800 parsecs.

It remains to note the effect of an error in the assumed absolute magnitude. If the mean absolute magnitude of the A stars is actually $+1^{M}0$ instead of $+0^{M}5$, the figures in Table IV should be decreased by something like 20 per cent and the resulting values of Δ correspondingly increased. An error of half a magnitude in the value of the absolute magnitude of the G stars has a much smaller effect.

I wish to thank Dr. van de Kamp and Dr. Vyssotsky for the opportunity of discussing this part of their material.

LEANDER MCCORMICK OBSERVATORY
UNIVERSITY OF VIRGINIA
December 1933

THE INTENSITIES OF STELLAR ABSORPTION LINES

By OTTO STRUVE and C. T. ELVEY

ABSTRACT

The intensities of stellar absorption lines have been measured in the spectra of α Canis Majoris, α Lyrae, α Cygni, α Persei, ϵ Aurigae and 17 Leporis. With the help of theoretical multiplet intensities, curves have been constructed, for each star separately, showing the relation between total absorption and number of atoms. These curves differ considerably. All parts of the curves lie between the limits $A = \text{Const.}$ and $A \propto N$.

An application of the theory of Schütz based upon the simultaneous effects of radiation damping and thermal Doppler broadening shows agreement with the observations in α Canis Majoris, α Lyrae, and α Cygni, provided, however, the damping constant is assumed to be ten times that given by the classical theory.

For the remaining three stars the hypothesis is advanced that in their atmospheres turbulent motions far exceed the motions caused by thermal agitation. The theory of Schütz is enlarged to include the case of turbulent motions, and excellent agreement with the observations is found.

The most probable turbulent velocity is found to be 67 km/sec. in 17 Leporis, 20 km/sec. in ϵ Aurigae, and 7 km/sec. in α Persei.

The interpretation of many other observational data in the light of the turbulence hypothesis is briefly discussed.

I. THE GRADIENT EFFECT

Several years ago Unsöld showed[1] that the theory of radiation damping could be applied to the wide wings of strong stellar absorption lines. The total absorptions of such lines increase in proportion to the square roots of the numbers of absorbing atoms. Essentially the same result has also been derived by J. Q. Stewart,[2] and applied by him, by Fairley[3] and by Korff,[4] to the sodium absorption lines in the sun and in the laboratory. Miss Payne[5] found from measurements of Harvard spectrograms that the square-root law is actually obeyed, over a wide range of spectral classes, in the case of the calcium lines H and K. For weak solar lines Minnaert[6] and Woolley[7] found departures from the square-root law which have since been explained by Minnaert and Mulders[6] on the basis of theoretical

[1] *Zeitschrift für Physik*, **44**, 793, 1927.

[2] *Astrophysical Journal*, **59**, 30, 1924.

[3] *Ibid.*, **67**, 114, 1928. [4] *Ibid.*, **76**, 124, 1932.

[5] *Harvard Observatory Circular*, No. 334, 2, 1928; *Proceedings of the National Academy of Sciences*, **14**, 404, 1928.

[6] *Zeitschrift für Astrophysik*, **1**, 192, 1930; **2**, 165, 1931.

[7] *Annals of the Solar Physics Observatory, Cambridge*, **3**, Part II, 1933.

developments by Schütz.[8] The latter showed that if the atoms of an absorbing gas are not quiescent but are subject to thermal agitation, the absorption coefficient as first derived by Voigt[9] gives a satisfactory explanation of the observed departures from the square-root law. For very faint lines the contours are essentially defined by the thermal Doppler effect. Radiation damping may be neglected when the number of atoms is small. Accordingly, the absorption coefficient is proportional to the number of atoms having any given velocity v, and the total intensity of the line increases proportionally to N. However, as the line becomes stronger, its central part becomes more and more saturated, causing a departure from the relation $A \propto N$, where A designates the total absorption. Were it not for radiation damping, A would become more and more independent of N, approaching a constant for large values of N. The effect of radiation damping prevents A from becoming a constant by producing wide wings which again permit A to increase with N. The ultimate result is again $A \propto \sqrt{N}$, as in the case of pure radiation damping.[10] A summary of the theoretical work on this problem has recently been published by Weisskopf.[11] Laboratory verifications are difficult and rest primarily upon measurements by Minkowski,[12] by Schütz,[13] and by Korff.[4]

The first application of Schütz's theory to astronomical spectra was made by Unsöld[14] in a discussion of the intensities of interstellar calcium lines. An even more convincing confirmation of the theory has been given by Minnaert and Mulders[6] for the faint lines in the sun's spectrum. Pannekoek,[15] and Minnaert and Slob,[16] have elaborated the theory of Schütz and made it directly applicable to stellar

[8] *Zeitschrift für Astrophysik*, **1**, 300, 1930; *Zeitschrift für Physik*, **64**, 682, 1930.

[9] *Sitzungsberichte der Akademie, München*, p. 602, 1912.

[10] This is correct only for values of N which are of practical significance. The formula for the absorption coefficient derived from the theory of radiation damping also demands $A \propto N$, for very small values of N (see Ladenburg and Reiche, *Annalen der Physik*, **42**, 181, 1913).

[11] *Physikalische Zeitschrift*, **34**, 1, 1933; *Observatory*, **56**, 302, 1933.

[12] *Zeitschrift für Physik*, **36**, 839, 1926. [13] *Loc. cit.*

[14] Unsöld, Struve, and Elvey, *Zeitschrift für Astrophysik*, **1**, 314, 1930.

[15] *Monthly Notices*, **91**, 139, 1930.

[16] *Proceedings of the Amsterdam Academy*, **34**, 542, 1931.

spectra. Pannekoek[17] has published measurements of line intensities in the spectrum of α Cygni and has interpreted these in the light of the theory as derived by Minnaert and Slob.

Total absorptions of certain multiplet lines have been measured by Shajn,[18] although the greater part of his work dealt with the central intensities. His conclusion was that real departures from the square-root law exist.

In 1930 the writers published a series of measurements[19] of the total absorptions of the *Si* III triplet λλ 4552, 4567, and 4574. The investigation was made principally to find whether the relative intensities in stars having nebulous lines are the same as those observed in stars having narrow lines. This was found to be the case, as had been predicted by the rotational hypothesis of broad and diffuse stellar absorption lines. It was also found that, on the average, the relative intensities were proportional to the square roots of the theoretical multiplet intensities derived from the rules of Burger and Dorgelo. There was found to be no marked difference between giants such as ζ Persei and dwarfs such as γ Pegasi.

In 1932 Struve[20] found a remarkable difference in the relative intensities of different members of multiplets in the stars 17 Leporis and ε Aurigae: while the strongest lines of *Fe* II and *Ti* II were slightly stronger in 17 Leporis than in ε Aurigae, the weaker lines were practically absent in the former though they were fairly strong in the latter. This phenomenon has been confirmed, from microphotometric measurements, by Hynek.[21]

New observational evidence of differences in the gradients of intensity of stellar absorption lines was announced by Struve and Morgan.[22] They found that the relative intensities of the members of the *Fe* I multiplet $a^3F - y^3F^o$ were not the same in several stars of classes A and F, and it was suspected that rotationally broadened lines had a tendency to possess smaller gradients. However, differ-

[17] *Ibid.*, p. 755. [18] *Monthly Notices*, **91**, 675, 1931.

[19] *Astrophysical Journal*, **72**, 267, 1930.

[20] *Ibid.*, **76**, 85, 1932; Pl. XI of this article contains a good illustration of the gradient effect. See also *ibid.*, **78**, Pl. VII, 1933.

[21] *Ibid.*, **78**, 54, 1933.

[22] *Proceedings of the National Academy of Sciences*, **18**, 590, 1932.

ences in the gradient could also be detected between stars having perfectly narrow lines.

The same investigators also found peculiar differences between the intensities of several *O* II lines in B stars. This subject was more fully investigated by Struve,[23] who found complete analogy between the phenomenon noted in 17 Leporis and ϵ Aurigae and the behavior of the *O* II lines. In a general way, all the stronger *O* II lines are greatly enhanced in the giants, while moderately faint lines appear to be of about equal intensity in giants and in dwarfs; the faintest *O* II lines are visible only in the dwarfs, such as τ Scorpii, and are not seen in the giants, such as β Canis Majoris.

It is true that the excitation potentials of the *O* II lines which are observed in stellar spectra are not all the same; they vary approximately between 23 and 31 volts. The intensities of the *O* II lines should, therefore, exhibit changes depending upon the degree of ionization, and such an effect has in fact been found by Struve.[24] However, a careful analysis of the lines, by multiplets, proves that the effect of gradient cannot be explained by differences in excitation. Consider, for example, the two multiplets shown in the accompanying tabulation. From the comparison of the intensities in τ

λ	Int. Lab.	Int. τ Sco (Dwarf)	Int. ϵ CMa (Giant)
	$e^4D^0-z^4F$		
4070	4+6	8	12
4072	8	6	10
4076	10	7	11
4079	4	3	3
4085	3	2	2
4093	5	2	1
	$e^4P^0-x^4P$		
4129	2	1	Blend
4133	6	5	3
4153	7	5	6
4156	3	3	1

[23] *Astrophysical Journal*, **78**, 73, 1933.

[24] *Op. cit.*, p. 83.

Scorpii and in ϵ Canis Majoris it appears reasonably certain that the strong lines are enhanced in the giant, while the weak lines are enhanced in the dwarf. This explains an interesting phenomenon repeatedly noticed in measuring the wave-lengths of stellar absorption lines: contrary to expectation, the faintest lines of any given element are not found in those stars in which the principal lines are strongest. One might, for example, be tempted to measure a star like ϵ Canis Majoris or β Canis Majoris in the hope of obtaining the faintest *O* II lines. In reality it is in the dwarf τ Scorpii that the greatest number of *O* II lines have been measured.[25]

The discovery of the gradient effect for *O* II made it desirable to reinvestigate the intensities of the *Si* III lines in B stars. Elvey's results[26] confirmed the earlier measurements,[19] but he found, in addition, that the gradient was not quite the same in all stars. Departures from the square-root law were generally in the direction of smaller gradients. The difference between giants and dwarfs is much less conspicuous than is the case for *O* II, but there is a slight tendency in the same direction. Thus we have:

For six giants: $\lambda 4552/\lambda 4567/\lambda 4574 = 41.3/35.2/23.5$
For six dwarfs: $\lambda 4552/\lambda 4567/\lambda 4574 = 40.6/33.6/25.8$

In examining the spectra of stars for the occurrence of the gradient effect, Morgan[27] found that ϵ Aurigae, the comparison star used by Struve and by Hynek in studying the gradient effect in 17 Leporis, was itself abnormal. A comparison with α Persei and 41 Cygni indicated that the gradient in ϵ Aurigae is much steeper than in the other two stars. ϵ Aurigae is a supergiant, while α Persei and 41 Cygni are normal giants of class F. It would be natural to expect an even smaller gradient in the dwarfs, but this is apparently not the case. Visual examination reveals no clear-cut difference in gradient between α Persei and a normal dwarf of the same spectral class.

On the other hand, Morgan[28] found striking differences in the intensity gradients of the *Fe* I lines in A-type stars. Thus, the peculiar star 73 Draconis shows a very small gradient, while in the normal A star ϵ Serpentis the gradient is larger. In the case of *Fe* I the intensities of the lines are correlated with excitation potentials, the

[25] For criteria of absolute magnitude in B stars we refer to earlier papers: O. Struve, *Astrophysical Journal*, **78**, 73, 1933, etc.

[26] *Ibid.*, p. 219. [27] *Ibid.*, p. 158. [28] *Ibid.*, **77**, 77, 1933.

fainter lines usually having slightly higher excitation potentials. It is improbable, however, that the differences noticed by Morgan are caused by normal excitation. Further work on the relative intensities of lines in A and F stars is now being carried out by Morgan and by Hynek, respectively.

The recognition of the gradient effect in many stars of different spectral classes makes it appear probable that other phenomena are directly or indirectly caused by it. Thus, the peculiar differences, noted by Struve,[29] of the singlet and triplet lines of *He* I are at least in part manifestations of the gradient effect. It so happens that the singlet lines are usually fainter than the corresponding triplet lines, consequently the conditions are suitable for the gradient effect. Whether all of the triplet-singlet differences can be accounted for in this manner has not yet been investigated.

An interesting manifestation of the gradient effect in the *He* I lines has recently been found by Morgan.[30] It appears that the variations of the intensities of the *He* I lines discovered by him in the spectroscopic binary μ Sagittarii[31] and by Struve in the spectroscopic variable 27 Canis Majoris[32] are simply changes in the intensity gradients. A similar effect is also present in the spectrum of β Lyrae.[30]

A first attempt to measure the differences in gradient of the lines of *Fe* II and *Ti* II has recently been made by Elvey.[33] His results confirmed the visual observations, but completely failed to give any clue to the cause of the variations. There was no definite correlation with either atomic number or spectral type, or even absolute magnitude of the stars.

The absence of a correlation with absolute magnitude was especially perplexing, because such a correlation had been rather definitely suspected for *O* II in the B stars. It had also been shown in the comparison of 17 Leporis, ϵ Aurigae, α Persei, and 41 Cygni. On the other hand, for *Si* III the absolute-magnitude effect was, if present at all, much smaller than were individual differences between stars of approximately the same luminosity.

The phenomenon is a complicated one, and the present investiga-

[29] *Ibid.*, **74**, 225, 1931; **78**, 73, 1933.

[30] Unpublished.

[31] *Astrophysical Journal*, **75**, 407, 1932.

[32] *Ibid.*, **73**, 301, 1931.

[33] *Ibid.*, **79**, 263, 1934.

tion is an attempt to explain it on the basis of the working hypothesis proposed in section IV.

II. THE OBSERVATIONS

A closer examination of the intensities of the lines of selected multiplets of *Fe* II and *Ti* II published by Elvey[33] indicated that the lines of both elements could be combined into one set showing a correlation between the total absorptions and the theoretical intensities. For three of the stars—α Persei, α Canis Minoris, and 41 Cygni—there was very little change in the total absorption, with a large change in the theoretical intensities, the total absorption varying with about the ninth root of the theoretical intensities. On the other hand, in α Cygni and α Lyrae the total absorption varied with the square roots of the theoretical intensities, and in 17 Leporis approximately with the theoretical intensities.

It is difficult to find a sufficient range in the intensities of the lines within a single multiplet to make satisfactory tests of the relationships between the theoretical and the observed intensities of absorption lines. The foregoing data showed, as have other data, that different multiplets can be combined to form relationships between the absorption and the number of atoms. Such combinations, covering a large range in intensities, tend to smooth over the irregularities exhibited by individual multiplets such as have been found by Woolley[7] and attributed by him to "interlocking." The foregoing data also indicate the course to be taken for further accumulation of observational material. Since the lines that have been observed are among the more intense lines in the spectrum of the particular star, and since there are such great differences among the various stars in the relationship between total absorption and theoretical intensity, it is desirable to obtain as much observational material in a given spectrum as is possible.

To accomplish this we have used the Bruce spectrograph with a dispersion of three prisms, the scale being 10 A/mm at λ 4500, to obtain spectrograms of some of the brighter stars on plates of high contrast. The emulsion used is Eastman O IV, and the developer was D-11. Because of the high contrast of the plates, it was necessary to make use of several spectrograms of each star, using different ex-

posures, in order to have satisfactory densities in the various parts of the spectrum for the accurate determination of the intensities.

Tracings of the spectrograms were made with the recording microphotometer, the magnification being about 30. Each part of the spectrum was run through the microphotometer a second time with a displacement of the plate by half a turn of the screw, to eliminate the periodic errors due to one turn of the screw. The central intensity of a line was measured in the usual manner and the total intensity was obtained by measuring the base of the line on the tracing and computing the area, assuming the line to have a triangular contour. The procedure is justified, since previous work[33] has shown no appreciable systematic differences, for lines of the intensities used in this investigation, between results obtained in this manner and those obtained by integrating the entire contour. The resulting total intensities are expressed in angstrom units of complete absorption of the continuous spectrum.

Practically all the measurements of intensity have been confined to those parts of the spectrum for which the tracings fell on the straight-line portion of the reduction-curve for the plate. The intensities in different parts of the spectrum were measured on different spectrograms, but there was sufficient overlapping to insure against systematic errors from plate to plate.

The resulting intensities for the five stars, α Canis Majoris, α Lyrae, α Cygni, α Persei, and ϵ Aurigae, are listed in Table I. The total absorptions in Angstrom units have been expressed as $\log A$. The measured wave-lengths and the identifications are partly by Morgan.[30] The tabulated wave-length is that measured in α Cygni, whenever available; when not, the wave-length in α Lyrae is given. In the identifications, only the most important contributor to the line has been listed, except where there is some uncertainty or where the blend is from two lines of about equal strength. In a few cases a line has been measured as single on the spectrogram, while on the tracing it was possible to sketch the shapes of two lines from the asymmetry of the contour and obtain a measure of the total absorption. In such cases the table gives a single wave-length for the blend, but separate intensities for the components. For example, the line λ 4227.01 is composed of the two lines *Ca* I 4226.73 and *Fe* I 4227.45, each of which has been measured.

TABLE I

λ	log A					Identification		
	α CMa	α Lyr	α Cyg	α Per	7 ε Aur			
4215.60	−0.93	−1.35	−1.28	.....	.....	*Sr* II	15.52	$5^2S-5^2P^o$
4217	1.58	.....	.....	.....	.....	*Fe* I	17.56	z^5F^o-9
4219.34	1.47	1.92	.....	.....	.....	*Fe* I	19.36	.....
4222.24	1.51	.....	.....	.....	.....	*Fe* I	22.23	$z^7D^o-e^7D$
4227.01	1.24	1.12	1.37	.....	.....	*Ca* I	26.73	$4^1S-4^1P^o$
	1.11	1.41	1.42	.....	.....	*Fe* I	27.45	z^5F^o-46
4233.05	0.80	0.91	0.25	.....	.....	*Fe* II	33.16	$b^4P-z^4D^o$
4235.62	1.17	1.62	2.05	.....	.....	(*Y* II	35.70)	$a^3D-z^3P^o$
						Fe I	35.95	$z^7D^o-e^7D$
4239.01	1.43	1.40	2.05	.....	.....	*Fe* I	38.83	z^5F^o-59
4242.32	1.05	1.48	0.76	.....	.....	*Cr* II	42.35	$a^4F-z^4D^o$
4244.62	.....	.....	2.00	.....	.....	*Ni* II	44.80	$a^2G-z^4F^o$
4245	1.62	.....	.....	.....	.....	*Fe* I	45.26	b^3P-20^o
4246.89	.....	.....	0.82	.....	.....	*Sc* II	46.83	$a^1D-z^1D^o$
4247.34	1.44	.....	.....	.....	.....	*Fe* I	47.44	z^5F^o-28
4250.19	1.22	2.22	1.85	.....	.....	*Fe* I	50.13	$z^7D^o-e^7D$
	1.21	1.35	1.58	.....	.....	*Fe* I	50.79	$a^3F-z^3G^o$
4252.60	1.42	1.88	1.39	.....	.....	*Cr* II	52.63	$a^4F-z^4D^o$
4254.53	1.15	.....	1.52	.....	.....	*Cr* I	54.34	$a^7S-z^7P^o$
4256.18	.....	.....	1.85	.....	.....	*Fe* I	56.21	z^5F^o-19
4258.21	1.37	.....	0.90	.....	.....	*Fe* II	58.16	$b^4P-z^4F^o$
4259.13	.....	.....	1.92	.....	.....	.....	.....	.....
4260.31	1.07	1.42	1.43	.....	.....	*Fe* I	60.49	$z^7D^o-e^7D$
4261.81	1.05	1.55	0.85	.....	.....	*Cr* II	61.91	$a^4F-z^4D^o$
4263.96	.....	.....	1.58	.....	.....	.....	.....	.....
4267.90	.....	.....	1.58	.....	.....	*Fe* I	67.83	.....
4269.26	1.36	.....	1.32	.....	.....	*Cr* II	69.30	$a^4F-z^4D^o$
4270.66	.....	.....	1.85	.....	.....	.....	.....	.....
4271.70	1.28	1.60	1.24	.....	.....	*Fe* I	71.17	$z^7D^o-e^7D$
	1.12	1.38		.....	.....	*Fe* I	71.76	$a^3F-z^3G^o$
4273.32	1.29	1.85	0.88	.....	.....	*Fe* II	73.31	$b^4P-z^4D^o$
4275.48	1.34	.....	.....	.....	.....	*Cr* I	74.80	$a^7S-z^7P^o$
	1.24	1.89	1.00	.....	.....	*Cr* II	75.55	$a^4F-z^4D^o$
4278.21	1.55	.....	1.13	.....	.....	*Fe* II	78.13	.....
4282.50	1.28	.....	.....	.....	.....	*Fe* I	82.41	$a^5P-z^5S^o$
4284.35	1.25	.....	1.06	.....	.....	*Cr* II	84.20	$a^4F-z^4D^o$
4286.39	.....	.....	1.72	.....	.....	*Zr* II	86.51	.....
4287.93	1.31	.....	1.17	.....	.....	*Ti* II	87.88	$a^2D-z^2D^o$
4290.27	1.51	.....	.....	.....	.....	*Cr* I	89.72	$a^7S-z^7P^o$
	1.10	1.04	0.66	.....	.....	*Ti* II	90.23	$a^4P-z^4D^o$
4294.12	1.12	1.14	0.77	.....	.....	*Ti* II	94.10	$a^2D-z^2D^o$
						Fe I	94.13	$a^3F-z^5G^o$
4296.54	1.12	.....	0.62	.....	.....	*Fe* II	96.56	$b^4P-z^4F^o$
4299.97	1.35	1.77	.....	.....	.....	*Fe* I	99.25	$z^7D^o-e^7D$
	0.92	1.04	0.52	.....	.....	*Ti* II	00.05	$a^4P-z^4D^o$
4301.91	1.17	1.47	0.96	.....	.....	*Ti* II	01.93	$a^4P-z^4D^o$
4303.28	1.02	1.21	0.56	.....	.....	*Fe* II	03.18	$b^4P-z^4D^o$
4305.67	1.57	1.85	.....	.....	.....	*Sr* II	05.46	$5^2P^o-6^2S$
						Fe I	05.46	$3M-z^3S^o$
4307.81	−0.90	−1.00	−0.79	.....	.....	*Ti* II	07.89	a^4P-z^4D
						Fe I	07.91	$a^3F-z^3G^o$

TABLE I—*Continued*

λ	log *A*					Identification		
	α CMa	α Lyr	α Cyg	α Per	7 ε Aur			
4309.66	−1.54	.....	.....	.....	.....	*Y* II	09.63	$a^3D-z^3P^o$
4312.79	1.08	−1.24	−0.96	.....	.....	*Ti* II	12.88	$a^4P-z^4D^o$
4314.18	1.32	1.38	0.77	.....	.....	*Sc* II	14.09	$a^3F-z^3D^o$
4314.87	1.00	1.40	0.97	.....	.....	*Ti* II *Fe* I	14.98 15.09	$a^4P-z^4D^o$ $a^5P-z^5S^o$
4316.87	.....	.....	1.55	.....	.....	*Ti* II	16.80	$b^2P-z^2P^o$
4320.85	1.54	.....	1.96	.....	.....	*Sc* II *Ti* II	20.73 20.95	$a^3F-z^3D^o$ $a^4P-z^4D^o$
4325.52	..... 0.84	.....	1.44 0.96	.....	.....	*Sc* II *Fe* I	25.00 25.77	$a^3F-z^3D^o$ $a^3F-z^3G^o$
4330.55	.....	.....	1.22	.....	.....	*Ti* II *Ti* II	30.25 30.71	$b^2P-z^2P^o$ $a^4P-z^4D^o$
4337.95	.....	.....	0.98	.....	.....	*Ti* II	37.92	$a^2D-z^2D^o$
4343.10	.....	.....	2.05	.....	.....	*Fe* I	43.27	.....
4344.21	.....	.....	1.24	.....	−0.26	*Ti* II *Cr* I	44.31 44.51	$a^2D-z^2D^o$ $a^5D-z^5F^o$
4347.83	.....	.....	.....	−1.05	.....	*Fe* I	47.85	$z^5P^o-f^5D$
4351.80	0.67	1.13	0.28	0.67	0.07	*Fe* II	51.77	$b^4P-z^4D^o$
4352.75	.....	.....	.....	0.84	.....	*Fe* I	52.74	$a^5P-z^5S^o$
4354.23	.....	.....	1.52	0.87	1.19	*Sc* II	54.60	$a^3F-z^3F^o$
4358.44	1.57	.....	.....	.....	.....	*Y* II *Fe* I	58.74 58.51	$a^3D-z^3P^o$ $b^3G-i^8^o$
4359.69	.....	.....	.....	0.90	1.13	*Zr* I	59.74	$b^4P-z^4D^o$
4362.02	1.48	1.46	1.48	.....	1.03	*Ni* II	62.10	$a^2G-z^4F^o$
4367.84	1.24	1.17	0.96	0.59	0.40	*Fe* I *Ti* II	67.58 67.67	$b^3G-z^3H^o$ $b^2F-y^2G^o$
4369.39	1.33	1.80	1.01	0.75	0.57	*Fe* II *Fe* I	69.41 69.78	$b^4P-z^4F^o$ $z^3F^o-f^3D$
4371.11	.....	.....	.....	0.77	1.16	*Zr* II	70.95	$b^4P-z^4D^o$
4373.6	.....	.....	.....	1.02	.....	*Fe* I	73.57	$b^3F-w^5D^o$ $b^3G-x^3F^o$
4374.67	1.05	1.64	1.07	.....	0.02	*Sc* II *Y* II	74.46 74.96	$a^3F-z^3F^o$ $a^1D-z^1D^o$
4379.86	.....	.....	.....	.....	0.97	*Zr* II	79.78	$a^2H-z^2G^o$
4383.48	0.84	1.03	0.96	.....	0.18	*Fe* I	83.55	$a^3F-z^5G^o$
4384.33	1.07	1.49	0.77	.....	.....	⊙ II *Mg* II	84.32 84.64	..... $4^2P^o-5^2D$
4385.40	0.97	1.33	0.58	.....	0.85	*Fe* II	85.39	$b^4P-z^4D^o$
4386.83	1.36	1.80	1.24	0.68	0.49	*Ti* II	86.84	$b^2F-y^2G^o$
4387.96	.....	.....	1.41	.....	.....	*Fe* I *He* I	87.90 87.93	$4M-z^3S^o$ $2P^o-5D$
4390.65	0.86	1.34	0.97	1.06	.....	*Mg* II *Fe* I	90.59 90.96	$4^2P^o-5^2D$ $b^3G-z^3H^o$
4391.0	.....	.....	.....	0.72	0.44	*Ti* II	91.02	$b^4P-z^4D^o$
4393.86	1.31	1.70	1.24	.....	.....	*Ti* II	94.06	$a^2P-z^4D^o$
4395.01	0.85	1.14	0.53	0.52	.....	*Ti* II	95.04	$a^2D-z^2F^o$
4395.84	.....	.....	.....	0.66	.....	*Ti* II	95.85	$b^4P-z^4D^o$
4398.08	.....	.....	.....	.....	0.67	*Y* II *Ti* II	98.03 98.31	$a^3D-z^3P^o$ $b^4P-z^4D^o$
4399.77	−1.17	−1.35	0.85	.....	.....	*Ti* II	99.77	$a^2P-z^4D^o$
4400	.....	.....	−1.51	−0.49	−0.08	*Sc* II	00.38	$a^3F-z^3F^o$

TABLE I—*Continued*

λ	log *A*					Identification		
	α CMa	α Lyr	α Cyg	α Per	7 ε Aur			
4403.28	.....	.....	.....	−1.00	−0.18	⊙ I	03.19	.....
						Zr II	03.33	$b^4P-z^4D^o$
4404.76	−0.88	−1.30	−1.35	.....	0.42	*Fe* I	04.75	$a^3F-z^5G^o$
4407.66	.....	.....	.....	.....	0.92	*Ti* II	07.68	$a^2P-z^4D^o$
						Fe I	07.72	$a^5P-x^5D^o$
4408.46	.....	.....	.....	0.71	.....	*Fe* I	08.42	$a^5P-x^5D^o$
4409.32	.....	.....	.....	0.61	0.63	*Ti* II	09.24	$b^4P-z^4D^o$
						Ti II	09.54	$b^4P-z^4D^o$
4411.12	1.36	.....	1.31	0.72	0.48	*Ti* II	11.08	$c^2D-x^2F^o$
4411.9	.....	.....	.....	0.91	1.05	*Ti* II	11.94	$b^4P-z^4D^o$
4414.47	.....	.....	.....	0.92	.....	*Zr* II	14.52	$b^4P-z^4D^o$
4415.37	1.01	.....	1.28	0.41	0.19	*Fe* I	15.13	$a^3F-z^5G^o$
						Sc II	15.55	$a^3F-z^3F^o$
4416.85	1.03	1.38	0.47	0.58	.....	*Fe* II	16.81	$b^4P-z^4D^o$
4417.70	1.09	1.39	0.96	0.94	.....	*Ti* II	17.71	$a^4P-z^2D^o$
4420.63	.....	.....	.....	0.92	.....	*Sc* II	20.66	$a^3F-z^3F^o$
4421.98	.....	.....	1.39	.....	0.35	*Ti* II	21.95	$b^2P-y^2D^o$
4425.45	.....	.....	.....	0.84	1.48	*Ca* I	25.43	$4^3P^o-4^3D$
4427.97	.....	.....	1.46	.....	1.00	*Ti* II	27.90	$b^4P-z^4D^o$
						Mg II	28.00	$4^2P^o-6^2S$
4430.61	.....	.....	.....	0.82	.....	*Fe* I	30.62	$a^5P-x^5D^o$
4431.37	.....	.....	.....	1.02	0.87	*Sc* II	31.35	$a^3F-z^3F^o$
4433.96	.....	.....	1.32	.....	.....	*Fe* I	33.81	z^5P^o-56
						Mg II	33.99	$4^2P^o-6^2S$
4434.80	.....	.....	.....	0.52	0.91	*Ca* I	34.95	$4^3P^o-4^3D$
						Fe I	35.15	$a^5D-z^7F^o$
4435.66	.....	.....	.....	0.62	.....	*Ca* I	35.67	$4^3P^o-4^3D$
4436.33	.....	.....	.....	1.30	.....	*Mn* I	36.36	$a^4D-z^4D^o$
4438.40	.....	.....	.....	1.57	.....	*Fe* I	38.36	$z^5P^o-f^5D$
4440.44	.....	.....	.....	0.94	.....	*Zr* II	40.44	$b^4P-z^4D^o$
4441.70	.....	.....	.....	.....	0.47	*Ti* II	41.72	.....
4443.84	.....	.....	0.55	.....	0.03	*Ti* II	43.80	$a^2D-z^2F^o$
4446.99	.....	.....	.....	1.02	.....	*Fe* I	46.85	$z^5P^o-f^5D$
						Fe I	47.14	.....
4447.76	.....	.....	.....	.....	1.16	*Fe* I	47.73	$a^5P-x^5D^o$
4450.44	.....	.....	0.94	0.39	0.11	*Ti* II	50.49	a^2D-z^2F
4451.60	.....	.....	1.27	0.83	.....	*Mn* I	51.58	$a^4D-z^4D^o$
4454.47	.....	.....	.....	1.09	.....	*Fe* I	54.39	$b^3P-x^3D^o$
4454.90	.....	.....	.....	0.27	0.63	*Ca* I	54.77	$4^3P^o-4^3D$
						Zr II	54.80	$a^2F-z^4G^o$
4455.30	.....	.....	1.19	.....	.....	*Ti* I	55.32	$b^3F-v^3F^o$
						Mn I	55.32	$z^6P^o-e^6D$
4455.89	.....	.....	.....	0.65	.....	*Ca* I	55.88	$4^3P^o-4^3D$
4456.33	.....	.....	.....	.....	0.91	*Ca* I	56.61	$4^3P^o-4^3D$
						Ti II	56.62	$c^2D-x^2F^o$
4459.20	.....	.....	.....	0.54	0.94	*Fe* I	59.13	$a^5P-x^5D^o$
4461.57	1.36	1.64	1.06	.....	0.69	*Zr* II	61.21	$a^2G-z^2F^o$
						Fe I	61.66	$a^5D-z^7F^o$
4464.45	1.62	1.58	1.09	.....	0.34	*Ti* II	64.47	$a^4P-z^2D^o$
4466.46	1.57	1.64	1.60	0.57	0.94	*Fe* I	66.56	$b^3P-x^3D^o$
4468.49	−0.97	−1.03	−0.54	−0.35	−0.48	*Ti* II	68.49	$a^2G-z^2F^o$

TABLE I—*Continued*

λ	log *A*					Identification		
	α CMa	α Lyr	α Cyg	α Per	7 ε Aur			
4470.88	−1.44	.....	.....	.....	−0.48	*Ti* II	70.88	$a^4P-z^2D^o$
4471.46	1.43	.....	−1.52	.....	.....	*He* I	71.48	$2^3P^o-4^3D$
						He I	71.69	
4472.94	1.39	.....	0.98	−0.58	0.62	*Fe* II	72.93	$b^4F-z^4F^o$
4475.90	1.39	−1.92	0.82	0.58	1.11	*Fe* I	76.02	$b^3P-x^3D^o$
4479.52	.....	.....	.....	1.15	.....	*Fe* I	79.61	$z^5P^o-f^5D$
4481.25	0.26	0.29	.....	.....	0.08	*Mg* II	81.13	$3^2D-4^2F^o$
						Mg II	81.33	$3^2D-4^2F^o$
4482.25	.....	.....	.....	0.53	.....	*Fe* I	82.18	$a^5D-z^7F^o$
						Fe I	82.26	$a^5P-x^5D^o$
4484.81	.....	.....	.....	0.88	.....	*Fe* I	84.24	$z^5P^o-f^5D$
4488.36	1.39	1.89	1.00	0.61	.....	*Ti* II	88.32	$c^2D-x^2F^o$
4489.19	1.17	1.48	0.62	0.47	.....	*Fe* II	89.21	$b^4F-z^4F^o$
4491.40	1.10	1.38	0.51	0.48	0.32	*Fe* II	91.41	$b^4F-z^4F^o$
4493.55	.....	.....	.....	.....	1.00	*Ti* II	93.52	$a^2D-z^4F^o$
4494.53	.....	.....	.....	0.55	0.95	*Fe* I	94.57	$a^5P-x^5D^o$
4496.79	.....	.....	.....	.....	0.88	*Zr* II	96.96	$a^2F-z^4G^o$
4499.04	.....	.....	.....	1.19	.....	*Mn* I	98.90	$a^4D-z^4D^o$
4501.28	1.08	1.10	0.52	0.35	0.06	*Ti* II	01.27	$a^2G-z^2F^o$
4502.25	.....	.....	.....	1.33	.....	*Mn* I	02.22	$a^4D-z^4D^o$
4508.29	0.97	1.10	0.30	0.46	0.14	*Fe* II	08.29	$b^4F-z^4D^o$
4512.79	.....	.....	.....	1.36	.....	*Ti* I	12.73	$a^5F-y^5F^o$
4515.37	1.05	1.17	0.37	0.49	0.30	*Fe* II	15.34	$b^4F-z^4F^o$
4517.64	2.15	.....	.....	.....	.....	*Fe* I	17.53	$4M-y^3P^o$
4518.36	.....	.....	.....	.....	0.83	⊙ II	18.34	.....
4520.21	1.08	1.28	0.40	0.49	0.27	*Fe* II	20.24	$b^4F-z^4F^o$
4422.65	1.03	1.26	0.33	0.33	0.19	*Fe* II	22.64	$b^4F-z^4D^o$
4524.99	.....	.....	1.70	.....	1.08	*Ti* II	24.72	$b^4P-z^2D^o$
						Fe I	25.15	z^5P^o-17
4526.35	.....	.....	.....	.....	1.60	*Fe* I	26.57	.....
4528.30	1.36	.....	.....	0.54	0.79	*Fe* I	28.62	$a^5P-x^5D^o$
4529.52	.....	.....	.....	0.54	0.59	*Ti* II	29.46	$a^2H-z^2G^o$
4534.04	0.90	1.05	0.44	0.24	0.10	*Ti* II	33.97	$a^2P-z^2D^o$
4541.53	1.31	1.48	0.58	0.54	0.39	*Fe* II	41.52	$b^4F-z^4D^o$
4544.06	.....	.....	.....	0.60	1.00	*Ti* II	44.01	$b^4P-z^2D^o$
4544.92	.....	.....	1.51	.....	0.94	*Ti* II	45.14	$a^2G-z^4F^o$
4549.53	0.54	0.71	0.14	.....	0.07	*Fe* II	49.48	$b^4F-z^4D^o$
						Ti II	49.64	$a^2H-z^2G^o$
4552.27	.....	.....	1.57	0.67	1.02	*Ti* II	52.29	$a^4G-z^4F^o$
						Fe I	52.55	
4554.02	.....	.....	.....	.....	0.45	*Ba* II	54.04	$6^2S-6^2P^o$
4554.96	1.29	1.82	0.83	.....	.....	*Cr* II	54.99	$b^4F-z^4D^o$
4556.00	1.13	1.28	0.38	0.37	0.15	*Fe* II	55.90	$b^4F-z^4F^o$
						Fe I	56.13	$b^3G-x^5G^o$
4558.66	0.99	1.28	0.36	0.53	0.32	*Cr* II	58.66	$b^4F-z^4D^o$
4563.79	1.11	1.24	0.50	0.42	0.10	*Ti* II	63.77	$a^2P-z^2D^o$
4565.77	1.66	.....	1.13	.....	0.86	*Fe* I	65.68	$z^5D^o-e^5F$
4568.33	.....	.....	.....	.....	1.12	*Ti* II	68.30	$b^4P-z^2D^o$
4571.97	1.03	1.17	0.50	0.26	0.16	*Ti* II	71.98	$a^2H-z^2G^o$
4576.36	−1.37	−1.96	−0.57	0.58	−0.39	*Fe* II	76.31	$b^4F-z^4D^o$
4578.56	.....	.....	.....	−1.01	.....	*Ca* I	78.57	$3^3D-4^3F^o$

TABLE I—*Continued*

λ	log *A*					Identification		
	α CMa	α Lyr	α Cyg	α Per	7 ε Aur			
4579.90	−1.27	.....	−0.88	.....	−0.63	.....	.....	.....
4581.42	.....	.....	.....	−0.84	.....	*Ca* I	81.41	$3^3D-4^3F^o$
						Fe I	81.53	$z^5D^o-e^3F$
4582.82	1.33	−1.82	0.55	0.45	.....	*Fe* II	82.84	$b^4F-z^4F^o$
4583.89	0.88	1.08	0.24	0.27	.....	*Fe* II	83.84	$b^4F-z^4D^o$
4585.92	.....	.....	.....	0.85	.....	*Ca* I	85.87	$3^3D-4^3F^o$
4588.19	1.15	1.62	0.38	0.52	0.32	*Cr* II	88.21	$b^4F-z^4D^o$
4589.85	1.54	1.96	0.89	0.48	0.47	*Ti* II	89.96	$a^2P-z^2D^o$
4592.03	1.27	1.92	0.72	0.44	0.64	*Cr* II	92.05	$b^4F-z^4D^o$
4593.92	.....	.....	1.92	.....	.....	.....	.....	.....
4595.90	1.64	.....	0.97	.....	1.04	*Fe* II	95.70	$b^4F-z^4D^o$
4598.22	.....	.....	1.42	0.85	.....	*Fe* I	98.14	$z^5D^o-e^5F$
4600.11	.....	.....	.....	.....	1.22	*V* II	00.20	.....
						Ni I	00.36	$z^5G^o-e^5F$
4601.33	.....	.....	.....	.....	1.28	*Fe* II	01.38	$a^6S-z^4D^o$
4605	1.74	.....	.....	.....	1.46	*Ni* I	04.99	$z^5G^o-e^5F$
4607.63	.....	.....	.....	0.91	.....	*Fe* I	07.67	$z^5D^o-e^5F$
4611.29	1.68	.....	.....	.....	.....	*Fe* I	11.29	z^5P^o-17
4616.69	1.17	.....	0.80	0.42	0.66	*Cr* II	16.67	$b^4F-z^4D^o$
4618.85	1.12	1.82	0.59	0.48	0.44	*Cr* II	18.82	$b^4F-z^4D^o$
4620.53	1.34	.....	0.78	0.44	0.61	*Fe* II	20.52	$b^4F-z^4D^o$
4625.02	.....	.....	.....	0.89	.....	*Fe* I	25.06	$z^5D^o-e^5F$
4626.07	.....	.....	.....	0.99	.....	*Cr* I	26.18	$a^5D-y^5P^o$
4629.34	1.08	1.64	0.33	0.37	0.23	*Fe* II	29.33	$b^4F-z^4F^o$
4634.05	1.12	−1.64	0.57	0.56	0.47	*Cr* II	34.12	$b^4F-z^4D^o$
4635.42	1.32	.....	1.01	.....	0.87	*Fe* II	35.35	.....
4637.50	.....	.....	.....	0.76	.....	*Fe* I	37.52	$z^5D^o-e^5F$
4638	.....	.....	.....	.....	1.23	*Fe* I	38.02	z^5P^o-31
4646.19	.....	.....	.....	0.70	1.24	*Cr* I	46.17	$a^5D-y^5P^o$
4647.41	.....	.....	.....	0.71	.....	*Fe* I	47.44	$b^3G-y^3G^o$
4648.74	.....	.....	.....	0.74	1.00	*Ni* I	48.66	$z^5G^o-e^5F$
4651.29	.....	.....	.....	1.17	.....	*Cr* I	51.30	$a^5D-y^5P^o$
4652.19	.....	.....	.....	1.15	1.62	*Cr* I	52.17	$a^5D-y^5P^o$
4654.56	.....	.....	.....	0.64	.....	*Fe* I	54.50	$a^3F-y^5F^o$
						Fe I	54.64	$z^5D^o-e^5F$
4657.04	1.26	.....	0.83	.....	0.49	*Fe* II	56.98	$a^6S-z^4D^o$
4661.94	.....	.....	.....	1.05	.....	*Fe* I	61.98	$b^3G-y^3G^o$
4663.30	1.21	.....	0.92	.....	0.79	*Fe* II	63.71	$a^6S-z^4F^o$
4664.81	.....	.....	.....	1.22	.....	*Cr* I	64.81	$z^7F^o-g^7D$
4666.76	1.26	.....	0.70	0.41	0.40	*Fe* II	66.75	$b^4F-z^4F^o$
4668.14	.....	.....	.....	0.61	.....	*Fe* I	68.15	$z^5D^o-e^5F$
4670.16	−1.55	.....	−0.99	.....	0.39	*Sc* II	70.40	$b^1D-z^1F^o$
4682.69	.....	.....	.....	.....	1.55	*Y* II	82.32	$a^1D-z^3P^o$
4686.13	.....	.....	.....	1.42	.....	*Ni* I	86.21	$z^5G^o-e^5F$
4691.44	.....	.....	.....	0.91	.....	*Fe* I	91.42	$b^3G-y^3G^o$
4698.69	.....	.....	.....	.....	1.01	*Sc* II	98.30	$a^3F-z^1D^o$
						Cr II	98.74	$a^4P-z^4F^o$
4702.97	.....	.....	.....	.....	1.03	*Mg* I	03.00	$3P^o-5D$
4707.31	.....	.....	.....	0.73	.....	*Fe* I	07.29	$z^5D^o-e^5F$
4708.75	.....	.....	.....	0.60	−0.72	*Ti* II	08.66	$a^2P-z^2F^o$
4710.17	.....	.....	.....	−1.12	.....	*Fe* I	10.28	$b^3G-y^3G^o$

TABLE I—*Continued*

λ	log *A*					Identification		
	α CMa	α Lyr	α Cyg	α Per	7 ε Aur			
4714.41	.....	.....	.....	−0.80	−1.51	*Ni* I	14.42	$z^5G^o-e^5F$
4715.81	.....	.....	.....	1.37	.....	*Ni* I	15.76	$z^5G^o-e^5F$
4718.41	.....	.....	.....	1.29	.....	*Cr* I	18.45	$z^7F^o-g^7D$
4719.8	.....	.....	.....	.....	1.13	*Ti* II	19.51	$b^4P-z^2F^o$
4731.32	.....	.....	−0.78	.....	0.44	*Fe* II	31.49	$a^6S-z^4D^o$
4736.89	.....	.....	.....	0.60	1.08	*Fe* I	36.79	$z^5D^o-e^5F$
4756.47	.....	.....	.....	0.90	.....	*Ni* I	56.53	$z^5G^o-e^5F$
4764.23	.....	.....	.....	.....	0.57	*Ni* I	63.95	$z^3F^o-f^3F$
4770.26	.....	.....	.....	.....	1.64	*C* I	70.00	$3s^3P^o-4p^3P$
4780.07	.....	.....	0.94	−0.61	0.53	*Ti* II	79.99	$b^2P-z^2S^o$
4783.17	.....	.....	.....	.....	1.42	*Mn* I	83.43	$z^8P^o-e^8S$
4786	.....	.....	.....	.....	1.42	*Y* II	86.58	$a^3F-z^3D^o$
4798.57	.....	.....	.....	.....	0.90	*Ti* II	98.52	$a^2D-z^4G^o$
4805	.....	.....	0.82	.....	0.42	*Ti* II	05.11	$b^2P-z^2S^o$
4812.11	.....	.....	1.15	.....	0.77	*Cr* II	12.37	$a^4F-z^4F^o$
4823.92	.....	.....	0.55	.....	0.30	*Cr* II	24.13	$a^4F-z^4F^o$
4836.38	.....	.....	1.06	.....	0.97	*Cr* II	36.23	$a^4F-z^4F^o$
4848.27	.....	.....	0.64	.....	−0.51	*Cr* II	48.27	$a^4F-z^4F^o$
4854.8	.....	.....	−1.49	.....	.....	*Y* II	54.89	$a^3F-z^3D^o$

Pannekoek[17] has measured the total absorptions of a number of lines of *Fe* II, *Ti* II, and *Cr* II in α Cygni, and a comparison between our measures and his shows a systematic difference of about 15 per cent, in the sense that our total absorptions are smaller than his (Fig. 1). Such a systematic error may result from differences in judgment as to the position of the continuous spectrum across a line and also in measuring the point where the contour of the line joins the continuous spectrum. For the narrow lines of the metals the latter is probably the source of the differences.

A comparison of the total absorptions with theory requires a knowledge of the emission intensities of the lines, since they are proportional to the numbers of atoms producing the lines. The laboratory intensities are unsatisfactory, largely owing to a lack of accurate photometric data. For a large portion of the lines the theoretical intensities are available from the formulae of Russell and of others, but these are only relative intensities within a given multiplet. We have made use of an investigation of the flash spectrum by Pannekoek and Minnaert[34] in which they have made a comparison of the intensities

[34] Results of observations of the total solar eclipse of June 29, 1927; photometry of the flash spectrum, Amsterdam, 1928.

observed in the flash spectrum with the theoretical intensities. They found linear relationships between the logarithms of the flash intensities and the logarithms of the theoretical intensities. These results were obtained by first plotting as ordinates the logarithms of the flash intensities and as abscissae the logarithms of the theoretical intensities for individual multiplets of an atom, and by then shifting the curves with respect to one multiplet along the abscissa until all points fell on a smooth curve, in this case a straight line. The amount of the shift of each multiplet relative to one chosen for zero point gives a correction to be applied to the logarithms of the intensities in that multiplet. Pannekoek and Minnaert do not give the corrections for all of the multiplets, so we have determined them from their data. These corrections are given in Table II and are in the form of the logarithms which must be added to the logarithms of the theoretical intensities given in their paper.

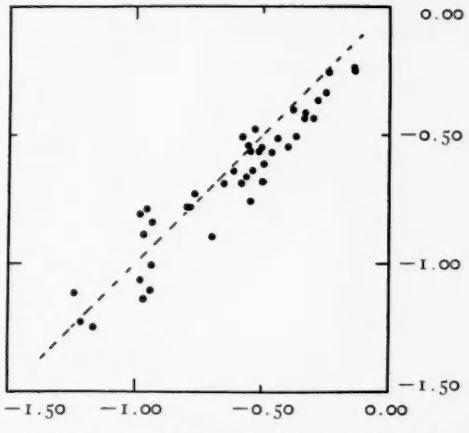

FIG. 1.—Comparison of Yerkes measures (ordinates) of log A for α Cygni with those of Pannekoek (abscissae).

This gives us a homogeneous set of theoretical intensities for each atom, which we can use for all the stars. To find the relationship between the total absorptions for a given star and the theoretical intensities of all of the lines, we have plotted as ordinate log A (total absorption) and as abscissa log E (theoretical intensity) for each atom. Since we have no information on the relative abundance of the atoms forming the lines in question, we must adjust empirically the curves for the various elements in exactly the same manner as for the multiplets in the flash spectrum. In all cases we have taken the *Fe* II lines as the basis for establishing the zero point. The plots for the various atoms were shifted until the best smooth curve was formed. The resulting curves are shown in Figures 2–6. Figure 7 is a curve for the star 17 Leporis constructed from data published by

Hynek.[21] There is some uncertainty about this curve since Hynek did not make accurate measures of the fainter lines. The five faintest lines plotted on the diagram are listed by him as "traces." In the discussion of this spectrum Hynek estimates the intensities of the lines which he called "traces" as 0.1 on his scale. Converting these into our scale of total absorptions, we obtain 0.05 A. We have compared these five lines in the spectrum of 17 Leporis with faint lines in other spectra which we have measured, and we feel confident that the adopted estimates of intensity are not greatly in error.

TABLE II

Fe I:		*Fe* II:	
$a^3F - z^3G^o$	−1.00	$b^4P - z^4D^o$	−0.55
$a^5P - x^5D^o$	−0.30	$b^4F - z^4F^o$	−2.00
$a^5P - z^5S^o$	+0.70	$b^4F - z^4D^o$	−1.60
$z^7D^o - e^7D$	−1.40	$b^4P - z^4F^o$	+0.20
$z^5D^o - e^5F$	−1.00		
Ca I:		*Ti* II:	
$4^3P^o - 4^3D$	0.00	$a^2D - z^2F^o$	+0.47
$4^3P^o - p^3P$	+0.20	$a^2D - z^2D^o$	+0.29
$3^3D - 4^3F^o$	+0.10	$a^2G - z^2F^o$	+0.10
		$a^2P - z^2D^o$	+0.53
		$a^2H - z^2G^o$	−0.38
		$a^4P - z^4D^o$	−0.74
		$a^2P - z^4D^o$	(−0.63)
		$b^4P - z^4D^o$	−2.25
		$b^2F - y^2G^o$	−1.86
Mn I:		*Sc* II:	
$a^4D - z^4F^o$	−0.60	$a^3F - z^3F^o$	−0.80
$a^4D - z^4D^o$	0.00	$a^3F - z^3D^o$	0.00
$a^4D - y^4P^o$	+0.80		
Cr I:		*Cr* II:	
$a^7S - z^7P^o$	+2.20	$b^4F - z^4D^o$	0.00
$a^5S - y^5P^o$	+0.70	$a^4F - z^4F^o$	−0.70
$a^5D - y^5P^o$	0.00	$a^4F - z^4D^o$	−0.90
$a^5D - z^5F^o$	−0.40		

III. SUMMARY OF OBSERVATIONAL DATA

From a comparison of the observational curves given in section II (Figs. 2–7) the following conclusions are derived:

1. The intensity gradient varies from star to star.

2. It is approximately constant in some stars. On the scales used in the figures the slope of the straight line is approximately 45° for α Cygni, 65° for 17 Leporis, 40° for Sirius, and 45° for Vega.

3. In other stars the gradient is variable. Thus, in α Persei and in ε Aurigae it is large for small values of N and A and decreases for large values of N and A. A slight amount of curvature in the opposite direction is suspected in the case of Sirius.

4. The gradient varies between extreme values of somewhat more than 0° and 65°, but it never exceeds the latter value. For the scales used the latter corresponds to $A \propto N$.

5. The gradient effect is not primarily a function of atomic number, excitation potential, or multiplet character, but depends, for each star, upon the total absorptions of the lines investigated.

6. We have made no attempt to study possible interlocking effects which may be present. Nor have we made a minute comparison of different elements in each star. We assert, merely, that the gradient effect is more pronounced than other effects. The work of Woolley and, more recently, that of Thackeray[35] indicate that there are real differences between multiplets, which are independent of the total absorptions of the lines considered. From a preliminary inspection of the data we are inclined to agree with them, and a more complete investigation of this phenomenon will be made at the Yerkes Observatory. In this paper we are concerned merely with the gradient effect obtained after smoothing over the results derived from many multiplets.

IV. THEORETICAL DISCUSSION

The theoretical work of Schütz, as elaborated by Pannekoek and by Minnaert and Slob, provides a good starting-point for the discussion. According to the latter,[36] thermal Doppler effect dominates the line contours for small numbers of atoms. For stars of temperature $T = 10{,}000°$ and for an element of atomic weight 50 (intermediate between *Fe* [56] and *Ti* [48]), the curve flattens out for lines the total absorptions of which are in the neighborhood of $A = 0.1$ A.

An inspection of our observed curves proves conclusively that this

[35] *Observatory*, **57**, 10, 1934; *Monthly Notices*, **94**, 99, 1933.

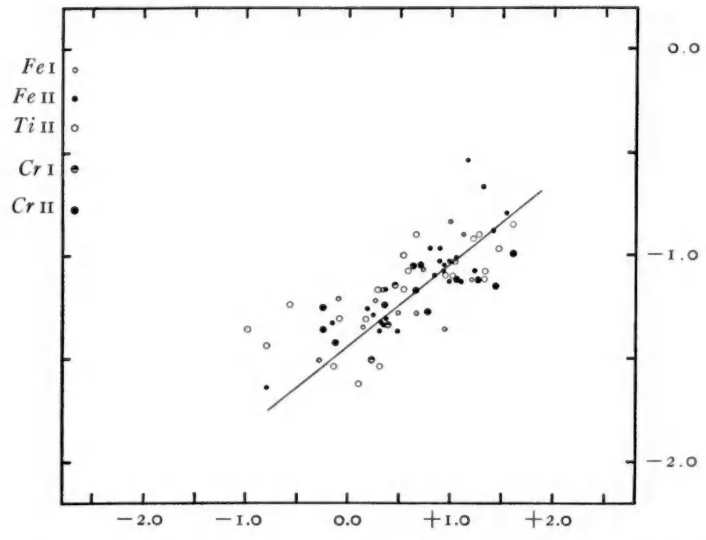

FIG. 2.—The variation of log A (total absorption) with log E (theoretical intensity) for lines in the spectrum of α Canis Majoris.

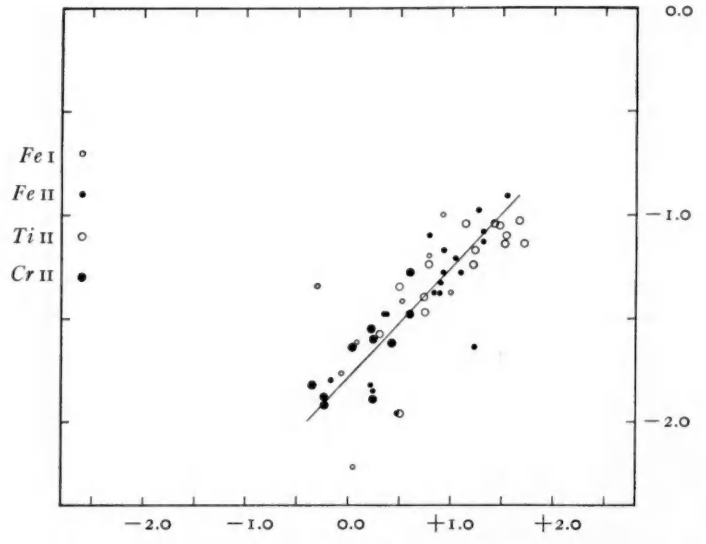

FIG. 3.—The variation of log A with log E for lines in the spectrum of α Lyrae

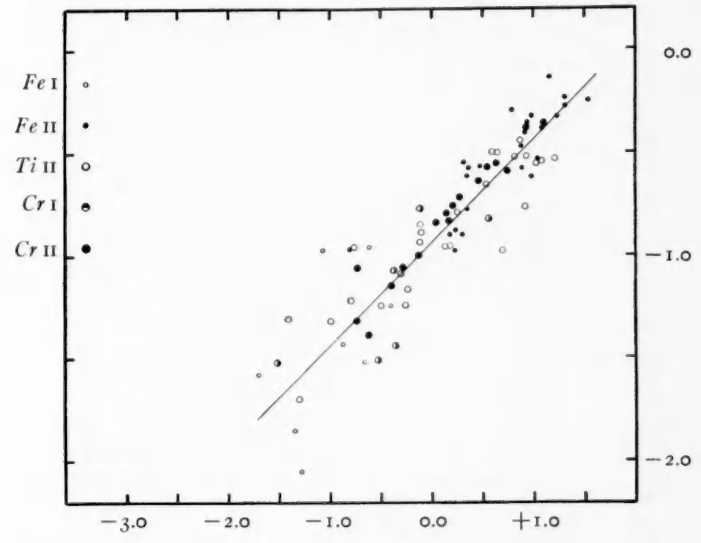

FIG. 4.—The variation of log A with log E for lines in the spectrum of α Cygni

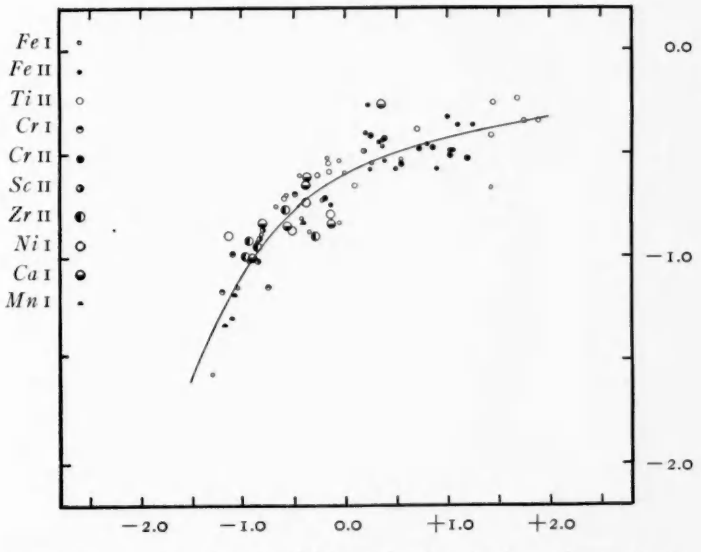

FIG. 5.—The variation of log A with log E for lines in the spectrum of α Persei

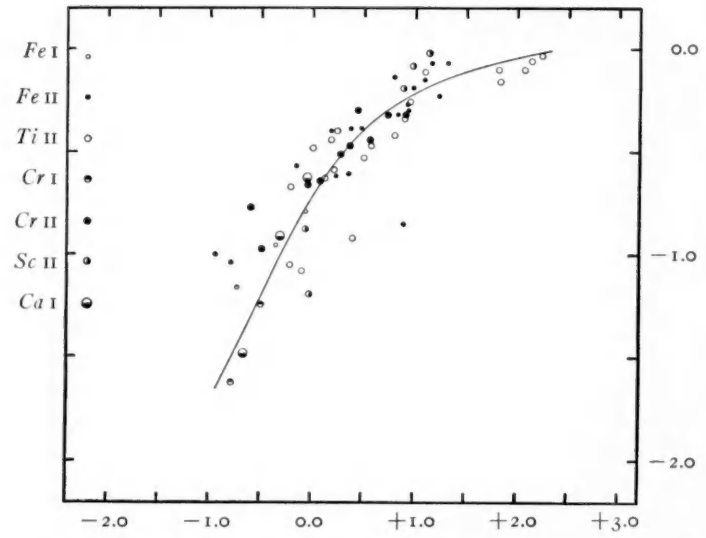

FIG. 6.—The variation of log A with log E for lines in the spectrum of ϵ Aurigae

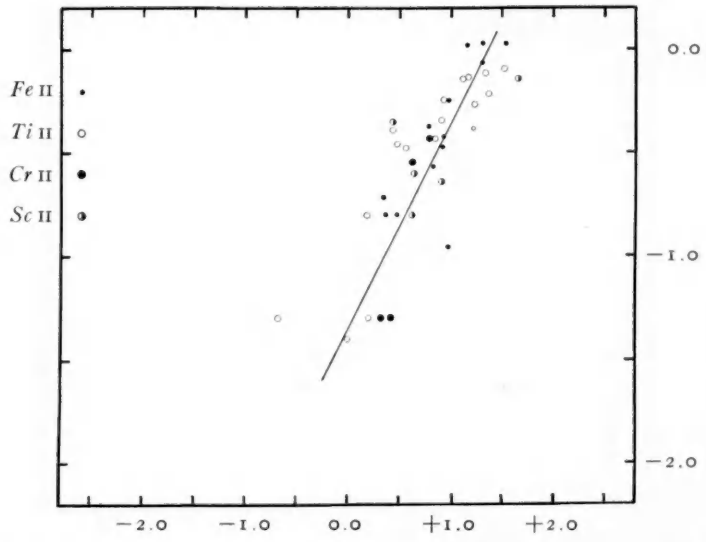

FIG. 7.—The variation of log A with log E for lines in the spectrum of 17 Leporis

is not true in all stars. In particular, 17 Leporis, ϵ Aurigae, and α Persei show a decided departure from the curve of Minnaert and Slob. In 17 Leporis the entire curve fits the relation $A \propto N$, over a range in A from 0.05 to 1.0 A. In ϵ Aurigae and in α Persei the shape of the curve resembles that of Minnaert and Slob, but the flat part of the curve is reached at about 1.0 A in ϵ Aurigae and at 0.4 A in α Persei.

In order to explain these departures we propose the following working hypothesis: The atmospheres of the stars are agitated not only by thermal motion of the individual atoms, but also by currents of a macroscopic character, which we shall refer to as "turbulence."

The possibility that turbulence is responsible for the gradient effect had already been tentatively considered by Struve and Morgan[22] and by Elvey,[33] but it is only with the help of the measures given in section II that a test of the hypothesis can be made.

We shall assume that the distribution of turbulent velocities is defined by Maxwell's law, and that consequently the absorption coefficient is [36]

$$\sigma = \frac{\sqrt{\pi}\,\epsilon^2 \lambda_0^2 N f}{mc^2 b}\, e^{-\left(\frac{\Delta\lambda}{b}\right)^2}, \tag{1}$$

where

$$b = \lambda_0 \frac{v_0}{c}$$

is the Doppler shift corresponding to the most probable turbulent velocity v_0. We have

ϵ = Charge of the electron
m = Mass of the electron
λ_0 = Wave-length of the center of the line
N = Number of atoms per cubic centimeter
f = Oscillator strength
c = Velocity of light

For the case of pure thermal agitation

$$b_0 = \frac{\lambda_0}{c}\sqrt{\frac{2RT}{M}}, \tag{2}$$

[36] A. Unsöld, *Astrophysical Journal*, **69**, 214, 1929.

where

R = Boltzmann constant
M = Atomic weight
T = Absolute temperature.

If thermal agitation and turbulence are both effective, b in formula (1) must be replaced by β, where

$$\beta = \sqrt{b^2 + b_0^2} .$$

For convenience we shall next assume that the reversing layer has a thickness H and that it absorbs exponentially:

$$I = I_0 e^{-\sigma H} . \tag{3}$$

This formula is not strictly correct, but the use of expressions more plausible theoretically, such as the Schuster-Schwarzschild approximation or the formula of Eddington,[37] does not appreciably alter the results, as was shown by Minnaert and Mulders[38] for the case of thermal agitation in the sun.[39] The total absorption of the line is

$$A = \int_{-\infty}^{+\infty} (1 - I) d\lambda .$$

The integral may be written in the form

$$A = 2 \int_0^{+\infty} \left(1 - e^{-ae^{-\frac{x^2}{b^2}}}\right) dx ,$$

where

$$a = \frac{\sqrt{\pi}\, e^2 \lambda_0^2 NfH}{mc^2 b} \, 10^8 = 10^{-13} \frac{NfH}{b} .$$

Introducing

$$\frac{x}{b} = y ; \qquad dx = b dy ,$$

[37] *Monthly Notices*, **89**, 620, 1929.

[38] *Zeitschrift für Astrophysik*, **2**, 171, 1931.

[39] In a private discussion Dr. D. H. Menzel has expressed the opinion that the use of eq. (3) may not be justified under the abnormal conditions prevailing in turbulent stellar atmospheres. This point should be further investigated.

we obtain

$$A = 2b \int_0^\infty \left(1 - e^{-ae^{-y^2}}\right) dy . \tag{4}$$

Expanding the exponential into a series, we obtain the following expression, which is convenient for small values of a:

$$A = 2\sqrt{\pi}\, ba \left\{ 1 - \frac{a}{2!\sqrt{2}} + \frac{a^2}{3!\sqrt{3}} - \cdots \right\} . \tag{5}$$

For large values of a this series is inconvenient, although it always converges. Professor Walter Bartky has derived for us the following asymptotic expansion[40] for large values of a:

$$A = 2b \left\{ \sqrt{\log_e a} + \frac{0.2886}{\sqrt{\log_e a}} - \frac{0.1335}{(\sqrt{\log_e a})^3} + \frac{0.0070}{(\sqrt{\log_e a})^5} + \cdots \right\} . \tag{6}$$

With the help of these two expansions we compute the theoretical values of A corresponding to different sets of NfH and b. The limiting straight lines have already been given by Unsöld.[14] They are

$$A = 1.8 \times 10^{-13} N \text{ (pure Doppler effect)} \tag{7}$$

and

$$A = 6.5 \times 10^{-9} \sqrt{N} \text{ (classical radiation damping)} . \tag{8}$$

Equation (8) has been found to be correct for ultimate lines, such as H and K of calcium. There is some doubt whether the constant is the same for subordinate lines. Indeed, Weisskopf and Wigner,[41] and also Oppenheimer,[42] have shown that the damping constant in the exact classical expression for the atomic absorption coefficient

$$\sigma = \frac{\gamma_{cl}}{(\frac{1}{2}\gamma_{cl})^2 + 4\pi^2(\nu - \nu_0)^2} ; \qquad \gamma_{cl} = \frac{8\pi^2 e^2 \nu_0^2}{3mc^3}$$

[40] Unpublished.

[41] *Zeitschrift für Physik*, **63**, 54, 1930; **65**, 18, 1931.

[42] *Physical Review*, **35**, 461, 1930. For a discussion of the absorption coefficient see D. H. Menzel, *Lick Observatory Publications*, **17**, 227, 1931.

is to be replaced by the following expression:

$$\gamma_{cl}=\frac{1}{T_n}+\frac{1}{T_m}=\sum A_n+\sum A_m ,$$

where T_n and T_m are the mean lifetimes of the atom in the upper and in the lower quantum states, and A_n and A_m are the corresponding transition probabilities. Since these quantities cannot, in general, be computed, the quantum-theoretical damping constant must be regarded as unknown. Minnaert and Mulders[6] found by computation that for certain lines the true damping constant could exceed the classical constant by a factor of 3 to 4.5. Actual measurements gave for the sun

$$\frac{\gamma_{obs}}{\gamma_{cl}}=9 .$$

Pannekoek[17] found for α Cygni a value of

$$\frac{\gamma_{obs}}{\gamma_{cl}}=19 ,$$

but since this result rests entirely upon the small amount of curvature shown in his Figure 3 (p. 762), which is not confirmed by our measurements (Fig. 4), we are inclined to consider it as relatively uncertain.

There remains the question whether the loss of energy through radiation is the only source of damping. The collisional damping of Lorentz which results from sudden changes in the phases of the oscillators may contribute an appreciable amount to the damping constant. Pannekoek[17] discarded collisional damping because his value of γ_{obs}/γ_{cl} for α Cygni was larger than Minnaert's for the sun. Since α Cygni is a supergiant, while the sun is a dwarf, the opposite should have been observed if collisional damping were effective. But if, for the reasons stated above, the curvature in Pannekoek's Figure 3 is spurious, this result no longer holds.

We shall assume that the damping constant is unknown, and write

$$\sigma_{obs}=C\sigma_{cl\ damp} .$$

Then for either the pure exponential absorption formula, or for the Schuster-Schwarzschild expression,[43]

$$A_{\text{damp}} = \text{Const.} \sqrt{C} .$$

Accordingly, an observed displacement of the limiting curve (8) along the axis of log A by an amount $\Delta \log A$ should lead to a determination of the damping constant:

$$\log \frac{\gamma_{\text{obs}}}{\gamma_{\text{cl}}} \approx \log C = 2\Delta \log A .$$

Figure 8 shows the integrand of formula (3) for different values of the parameter a. This illustrates the contours of lines broadened by

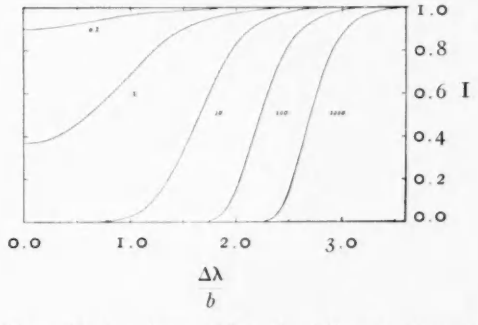

FIG. 8.—Theoretical contours of lines for different values of a

turbulence. Figure 9 shows the theoretical curves $A = \varphi\ (NfH)$ for $b = 1$, $b = 0.1$, and $b = 0.01$. The dotted line for $b = 0.03$ corresponds to a temperature of roughly 10,000° K. The limiting straight line on the right side of the diagram corresponds to the classical theory of radiation damping. Parallel to it run two other straight lines corresponding to $C = 4$ and $C = 10$, respectively. Figure 10 shows comparisons between theoretical and observed curves. For completeness we have included the average curve derived by Minnaert and Mulders for the sun. We see that the agreement is excellent if we assume that the three stars 17 Leporis, ϵ Aurigae, and a Persei have turbulent atmospheres, while in the sun, a Cygni, Vega, and Sirius, turbulence is not appreciable.

[43] O. Struve, *Monthly Notices*, **89**, 584, 1929.

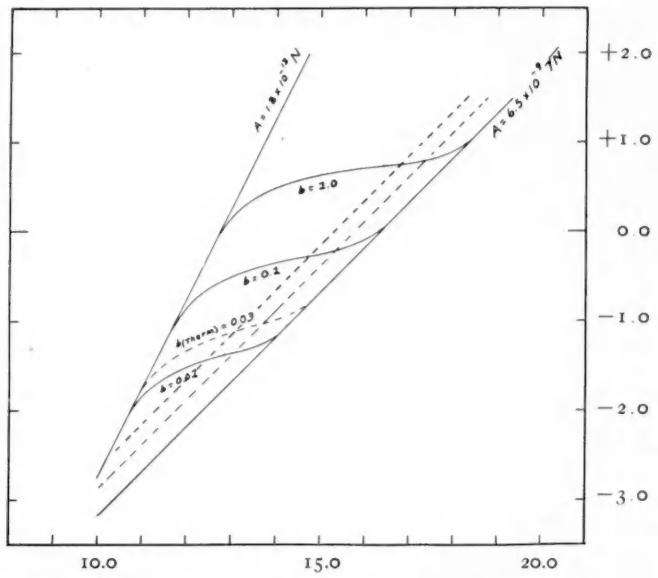

FIG. 9.—Theoretical relations between log A and log N

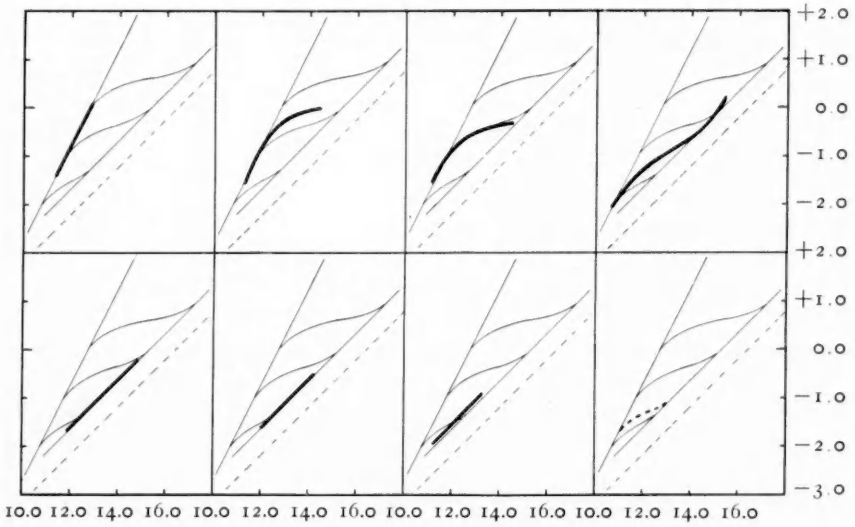

FIG. 10.—A comparison of the observed variations of log A with log E and of the theoretical variations. Upper row: 17 Lep., ϵ Aur., α Per., and Sun. Lower row: α Cyg., α CMa., α Lyr., and the theoretical curve for a temperature of 10,000° K. The theoretical curves are for a damping constant of ten times the classical value.

Estimating for each of the stars the value of b, we derive their average turbulent velocities. We can also compute the theoretical line widths from

$$e^{-ae^{-\frac{x^2}{b^2}}} = 0.5 .$$

For the last three stars a similar computation has been made on the basis of pure radiation damping:

$$e^{-C\frac{2\pi e^4 \lambda^2 NfH}{3m^2c^4x^2}} = 0.5 .$$

The values of NfH used in the computations were taken from the curves of Figure 10 and refer to the strongest lines measured in each

TABLE III

Star	b	v_0 Turb. Vel. or Therm. Vel.	Fictitious Temperature ($M=50$)	Line Width		
				Computed		Observed
				Turbulence	Rad. Damping	
17 Lep	1.0 A	67 km/sec.	3×10^7	1.2	.....	1.5
ϵ Aur	0.3	20	2×10^6	1.1	.....	1.0
α Per	0.1	7	3×10^5	0.5	.....	0.6
α Cyg	(0.03)	(2)	(10^4)	0.2	0.5	0.8
α CMa	(0.03)	(2)	(10^4)	0.1	.1	(0.5)
α Lyr	(0.03)	(2)	(10^4)	0.1	0.1	(0.4)
Sun	(0.03)	(2)	(10^4)	.....	.....	.....

star. The results given in Table III are surprisingly good for 17 Leporis, ϵ Aurigae, and α Persei. In all three stars an appreciable amount of broadening, produced by turbulence, is actually observed. In α Cygni the measured widths exceed the computed ones, although the character of the lines does not suggest rotation. For α Canis Majoris and α Lyrae the resolving power of the spectrograph is insufficient. The "fictitious temperature" is derived from (2) and merely shows what the temperature would have to be in order to produce the required values of b.

The curves for α Cygni, α Canis Majoris, and α Lyrae agree re-

markably well with the law $A \propto \sqrt{N}$, and there is no evidence of turbulence in these stars. Their curves have been shifted parallel to themselves, toward smaller values of log NHf, so as to obtain the best possible fit with the theory of Schütz. This is obtained for $C = 10$. A larger value of C is irreconcilable with the curves for α Persei and for the sun. A smaller value is inconsistent with the theory of Schütz. Even for $C = 10$, the lower parts of the observed curves $A = \varphi(NHf)$ fail to flatten out, as might be expected from the thermal curve shown in the last section of Figure 10. This might be construed to mean that, unless Schütz's theory is in error, thermal agitation is less pronounced than might be expected from the effective temperatures of these stars. While this may be true, it should be remembered that the lines are faint and difficult to measure, and that the highly unsatisfactory procedure of fitting each multiplet and each element into the best smooth curve may easily introduce errors into the curves. Because of this inherent uncertainty we have intentionally drawn straight lines for all stars except ϵ Aurigae and α Persei, in which the curvature was too large to be ignored.

We have assumed here that C is constant for all stars. In reality, it probably varies from multiplet to multiplet, producing a scatter in our observations. It may also vary from star to star, especially if collisional damping is not negligible. However, as a first approximation, our result $C = 10$ may be considered an average value[44] for the multiplets listed in Table II.

V. A POSSIBLE OBJECTION

The measured intensities for 17 Leporis, ϵ Aurigae, and α Persei agree remarkably well with the proposed theory, However, in 17 Leporis a visual inspection of the three lines of *Fe* I, λλ 4045, 4063, 4071, which are very faint, suggests that for these members of the $a^3F - y^3F^0$ multiplet the gradient is smaller than would be expected if $A \propto N$. In fact, all three lines are faintly visible, and the difference between λ 4045 and λ 4071 is small. Ordinary eye-estimates are deceptive, and it is possible that accurate measurements would show that the theory is obeyed. Unfortunately we are unable, with our

[44] Since the curve for the sun by Minnaert and Mulders has been used in our Fig. 10, this value is not quite independent of their result: $C = 9$.

present equipment, to obtain high-contrast spectra of sufficient dispersion for accurate measurement.

Nevertheless it is wise to consider the possibility that for these lines the gradient is smaller than is required by the law $A \propto N$. It is our opinion that even if this should be the case, it would not invalidate the theory. Our reasons are:

1. As explained in section III, individual multiplets may have peculiar gradients.

2. The steep gradient for all measurable lines of 17 Leporis is well established.

3. The almost complete absence of very faint lines shows that the theory is essentially correct.

4. In the star 17 Leporis turbulence is highly probable, as has been shown by Struve.[20] The absorption lines for which the gradient is large result from several shells which expand with different velocities, so that the combined effect is that of turbulence. The great width of the lines and the steep gradient are thus immediate consequences of the general behavior of the star.

5. It is not impossible that a theoretical explanation could be found for the occurrence of small gradients in the faintest lines.

VI. SUMMARY

With certain reservations (more completely explained in the preceding section), the proposed hypothesis of turbulent motions which in some stars tend to raise the flat portions of the curves $A = \varphi(NfH)$, provides a satisfactory extension of the theory of Schütz. The latter appears fairly well established from the work of Minnaert and his associates, on the sun, and of Dunham, on stars.[45] Our results for stars in which turbulence is inappreciable agree with this theory fairly well if the observed damping constant is taken to be approximately ten times that derived from the classical electron theory.

In pursuing farther the hypothesis of turbulent motions we conclude that B stars in which the gradients of the *O* II lines are large have turbulent atmospheres. Since such stars give curved lines for

[45] *Publications of the American Astronomical Society*, **7**, 215, 1933; W. S. Adams, "Summary of the Year's Work at Mount Wilson," *Publications of the Astronomical Society of the Pacific*, **45**, 279, 1933.

the relation $A = \varphi(NfH)$, it is quite possible that the gradients for the relatively weak *O* II lines will be large, while those for the *Si* III lines will be relatively small.

In fact, there is no definite answer to the question: What is the effect upon the gradient if we pass from a quiescent atmosphere to a turbulent one? If *NfH* remains constant, the gradient will either increase or decrease, depending upon whether we are nearer to the Doppler-effect branch or to the radiation-damping branch. But, if *NfH* changes, as is likely to be the case if the quiescent atmosphere is that of a dwarf while the turbulent atmosphere belongs to a giant, no answer can be given unless the actual change in *NfH* is known.

In several earlier papers Struve,[46] and Struve and Dunham,[47] concluded that in several B-type stars the lines were so narrow as to exclude the possibility of any appreciable turbulence. In fact, thermal Doppler effect was found to be practically sufficient to explain the observed line widths in such stars as τ Scorpii and γ Pegasi. This agrees well with our new results; these stars are typical dwarfs and their gradients suggest absence of turbulence.

On the other hand, the giants, such as ϵ Canis Majoris, have slightly broadened lines. In *some* of these stars axial rotation may be present, but the fact that *all* stars having large gradients have slightly broadened lines is highly suggestive. It is improbable that the axes of all these stars are oriented in such a way as to produce widening of the lines. The hypothesis of turbulence is much more satisfactory.

It should be remembered in this connection that rotational broadening does not change the gradient.[48] No observations have as yet been made of the gradients in stars showing large rotational velocities.

The idea of turbulence in the outer atmospheres of the stars is not new. Unsöld,[36] and after him Keenan,[49] have explained various phenomena in the solar chromosphere on the basis of turbulence. Even the aspect of the chromosphere with its prominences suggests turbulence in at least the outermost layers of the sun's atmosphere.

[46] *Proceedings of the National Academy of Sciences*, **18**, 585, 1932.

[47] *Astrophysical Journal*, **77**, 321, 1933.

[48] Struve and Elvey, *ibid.*, **72**, 267, 1930; *Monthly Notices*, **91**, 664, 1931.

[49] *Astrophysical Journal*, **75**, 277, 1932.

An appreciable effect of turbulence upon stellar absorption lines has been suspected by Menzel[50] in Cepheid variables, and by Adams and St. John[51] in several bright stars whose spectra revealed differences in the radial velocities obtained from enhanced lines and from arc lines. There is no obvious correlation between the results of Adams and St. John and those reported in this paper, but the methods used are so different that this is not surprising.

Finally, attention may be directed to a series of investigations by P. Guthnick,[52] who has attempted to explain by turbulence a number of peculiar phenomena in the radial velocities of such stars as α Lyrae and ϵ Ursae Majoris.

Whether all manifestations of the gradient effect may be explained on the basis of the enlarged theory of Schütz is not certain. For example, it is quite possible that there are also real differences between *He* I singlets and triplets, in addition to those reduced to the gradient effect. But many interesting results already suggest themselves. Among these are the following:

1. There is a tendency for very luminous stars to have larger turbulent velocities than are observed in less luminous stars.

2. There is, however, no *close* correlation between luminosity and turbulence, because some of the most notable supergiants show no turbulence.

3. The greatest amount of turbulence yet recorded is in the star 17 Leporis, which is peculiar in many other respects.

4. If turbulence is responsible for the variation of gradient in μ Sagittarii and in 27 Canis Majoris, we must conclude that the turbulent motions are not constant in these stars, or that *NfH* varies in such a manner as to imitate a change of gradient. Either explanation may be reasonable. In μ Sagittarii the largest gradient is observed a short time after periastron passage.

5. The extremely small gradient in the A-type star 73 Draconis is perplexing. There is no obvious reason why this star should have a turbulent atmosphere.

[50] *Publications of the American Astronomical Society*, **6**, 370, 1930.

[51] *Astrophysical Journal*, **60**, 43, 1924.

[52] *Sitzungsberichte der Preussischen Akademie der Wissenschaften: Phys.-math. Klasse*, **29**, Part II, Berlin, 1931.

6. It would be interesting to test the hypothesis of turbulence in novae, where the absorption lines may be broadened by uneven velocities of expansion of the shell.

7. Unfortunately none of the three turbulent stars investigated here is suitable for a study of their H and K lines. Theoretically, these lines, in at least the cooler stars, should lie on the right-hand branch of the curve, where $A \propto \sqrt{NfH}$, but blending with $H\epsilon$ makes measurements for *Ca* H uncertain.

8. The influence of the gradient effect upon the interpretation of absolute-magnitude effects is obvious and must be carefully investigated.

9. An investigation of separate multiplets and of the relative intensities of different multiplets of one element should be of interest.

10. We are inclined to think that the turbulence effect is most frequently observed in the hotter stars. It seems to be common in the B's and much rarer in the A's and the F's. In our observational work, 17 Leporis and ϵ Aurigae were not picked at random. Had we relied on a random selection of bright A and F stars, α Persei would have been the only one to show the gradient effect clearly.

YERKES OBSERVATORY
January 1934

NOTE ON BRUNT'S FORMULA FOR NOCTURNAL RADIATION OF THE ATMOSPHERE

By C. L. PEKERIS

ABSTRACT

It is shown that the linear dependence of the downgoing radiation of the atmosphere on the square root of the surface vapor pressure, discovered empirically by Brunt, can be explained by Dennison's theory of the shape of infra-red absorption lines. The theory is substantiated by Fowle's measurements of the total absorption in the bands 0.8 μ, ρ, and Φ of water vapor.

When a black surface is exposed to the free atmosphere on a clear night, its temperature drops because of the net loss of heat by radiation. The temperature drop is greater the drier the air, since the principal atmospheric radiating element is water vapor. This net loss of heat by radiation is usually measured by heating the black surface electrically until it assumes the temperature of the air. It is thus possible also to determine the downward radiation of the atmosphere and to correlate it with the moisture content and temperature of the surface layer.

It has recently been shown by D. Brunt[1] that the downward radiation R of the atmosphere on clear nights, when the vapor pressure (in millibars) and the absolute temperature in the surface layer are p and T respectively, can be represented, in the mean, by

$$R=\sigma T^4(a+b\sqrt{p}) , \tag{1}$$

$\sigma(=8.22\times10^{-11}$ gr. cal/min. cm^2) being the Stefan-Boltzmann constant and a and b empirical constants. The agreement of (1) with observations is very satisfactory, as can be seen, for example, from Table I, which is taken from Brunt's paper. It is based on a total of 1350 observations made by M. Robitzsch[2] at Lindenberg. The last column gives values computed from

$$\frac{R}{\sigma T^4}=0.342(1+0.37\sqrt{p}) . \tag{2}$$

[1] *Quar. J. R. Met. Soc.*, **58**, 389, 1932.

[2] *Arb. Preuss. Aeron. Obs., Lindenberg*, **15**, 203, 1926.

The coefficient of correlation between $R/\sigma T^4$ and $\sqrt{p}$ is 1.0. Similarly, a series of twenty-eight observations on clear nights made by S. Asklöf at Upsala[3] can, according to Brunt, be represented by

$$\frac{R}{\sigma T^4}=0.43(1+0.19\sqrt{p})\,. \tag{3}$$

The coefficient of correlation between $R/\sigma T^4$ and $\sqrt{p}$ is 0.83. On the other hand, the formula, due to A. Ångström,[4] by which Asklöf represents his observations,

$$\frac{R}{\sigma T^4}=A-B10^{-\gamma p}\,, \tag{4}$$

while apparently satisfactory, gives a correlation between computed and observed values of only 0.43. Brunt also shows that all the available data, which were obtained in various parts of the world

TABLE I

T	p^*	R	T^4	$\sqrt{p}$	$(R/\sigma T^4)$	$(R/\sigma T^4)$ Computed
303.2	16.0	0.601	0.700	4.0	0.859	0.851
301.2	14.5	.561	.682	3.8	.823	.825
299.6	13.5	.633	.668	3.6	.798	.800
294.4	12.3	.486	.622	3.5	.782	.787
290.4	11.6	.455	.590	3.4	.771	.774
287.8	10.2	.423	.570	3.2	.743	.749
285.6	9.6	.407	.552	3.1	.738	.736
281.0	7.5	.354	.517	2.7	.685	.685
279.3	5.5	.321	.505	2.3	.636	.634
276.6	4.3	.294	.485	2.1	.607	.609
269.1	2.5	0.246	0.435	1.6	0.566	0.545

* p in Table I and equation (2) is expressed in terms of millimeters. When millibars are used, the coefficient of $\sqrt{p}$ in (2) becomes 0.32, as is shown in Table II.

and at various elevations, can be well represented by formulae of type (1), the constants a and b differing, however, from place to place, as is shown in Table II. The variation in these constants Brunt attributes partly to the difference in instrumental constants used by various observers and to the effect of local topography on the mean variation of water vapor with height during the night.

[3] *Geogr. Ann. Stockholm*, **2**, 253, 1920.

[4] *Smiths Misc. Coll.*, **65**, No. 3, 1918.

Now equation (1), which is of a purely empirical nature, implies clearly that the nocturnal downward radiation of the atmosphere at a given locality (1) is determined, in the mean, by the surface temperature and vapor pressure; (2) varies as the fourth power of the temperature and linearly in the square root of the vapor pressure; and (3) that part of this radiation originates from sources other than water vapor.

This last effect was brought out long ago by A. Ångström's[4] extensive measurements. He accounts for it[5] by the long-wave radiation of the ozone which is known to exist at a mean height of about 50 km. This long-wave radiation, especially in the region of 9.1–10 μ,

TABLE II

Observer	Place	Elevation (Meters)	a	b	b/a	Correlation Coefficient
Dines	Benson	0	0.52	0.065	0.125	0.97
Asklöf	Upsala	0	.43	.082	.19	.83
Ångström	Bassour	1160	.48	.058	.12	0.73
Boutaric	Montpellier	2859	.60	.042	.07	.....
	Pic du Midi					
Robitzsch	Lindenberg	0	0.34	0.110	0.32	1.0
Mean	.....	.....	0.47	0.072	.....	.....

is readily transmitted by water vapor, and is thus registered at the ground. Another source of long-wave radiation, which is partly masked, however, by the concurring water-vapor emission, is the emission of CO_2. One must also consider the possibility that some of the earth's radiation, particularly of wave-lengths for which water vapor is transparent, is scattered downward by atmospheric dust which is abundant in the surface layers. The temperature of the ground would be expected to be more closely related to this radiation, as is demanded by (1), than to the radiation from the ozone layer. We should, however, put less emphasis on the temperature factor than on the dependence upon vapor pressure, because the variation of the latter is considerably greater than that of the former.

That the radiative power of the atmosphere on a clear night should be largely determined, in the mean, by surface conditions would be

[5] *Gerlands Beitr. Geophys.*, **21**, 145, 1929.

expected from the known absorption spectrum of water vapor and the conditions in the inversion layer. The absorption spectrum of water vapor is normally characterized by regions of strong and of very weak absorption. The bulk of the atmosphere's radiation originates therefore in the surface layers, as was exhibited quantitatively by G. C. Simpson[6] and D. Brunt.[1] In these layers the temperature becomes uniform in the early part of the night, owing to the cooling of the ground. Moreover, the subsequent quenching of turbulence helps to maintain the daytime status of a uniform distribution of moisture with height.

We are thus led to investigate the emission of an infinite horizontal slab of gaseous material (water vapor) of uniform temperature T and of mass M (in grams) in a vertical column of unit cross-section. In our particular application the gas rests on a black surface of the same temperature. The question arises whether the gas will be in a state of local thermodynamic equilibrium.[7] More precisely, may we expect that the distribution of molecules over two states differing in energy by ΔE will be given by

$$\frac{n_2}{n_1}=\frac{g_2}{g_1}e^{-\frac{\Delta E}{\kappa T}}, \tag{5}$$

g_2 and g_1 being the respective weights of the states. At the relatively high densities near the ground (5) is certainly obtained; there certainly exists a temperature and a Maxwellian distribution over energy. It follows[8] that the ν-radiation from the atmosphere incident on the ground per unit area is

$$\pi I(\nu,T)\left[1-e^{-\beta}(1-\beta)-\beta^2\int_\beta^\infty \frac{e^{-x}}{x}\,dx\right], \tag{6}$$

$$\beta=k_\nu M ,$$

where $I(\nu, T)$ is black-body radiation for the given frequency and temperature, and k_ν the coefficient of absorption. To get the total emission we must integrate (6) over all frequencies, and for that we have to know k_ν as a function of frequency. This question was treat-

[6] *Mem. R. Met. Soc.*, **3**, No. 21, 1928.

[7] E. A. Milne, *Handbuch der Astrophysik*, **3** (1st Half), Part III, 97, 1930.

[8] *Ibid.*, p. 85.

ed by D. M. Dennison[9] and was also dealt with by Brunt in the above-mentioned paper. Dennison finds that for a given rotational line, k_ν is given by

$$k_\nu = \frac{a}{b+(\nu-\nu_0)^2}, \tag{7}$$

where a and b are constants proportional respectively to $\sqrt{T}$ and $\rho^2 T$, ρ being the density. Since, then, the frequency interval over which k_ν is appreciable is small, we may consider $I(\nu, T)$ constant over that interval and keep it outside the integral sign. Putting $\nu-\nu_0=x$, we obtain from (6)

$$\left.\begin{aligned} \pi I_k(T) &= \pi I(\nu_0, T)\int_{-\infty}^{\infty}\left[1-e^{-\frac{aM}{b+x^2}}\left(1-\frac{aM}{b+x^2}\right)-\left(\frac{aM}{b+x^2}\right)^2\int_{\frac{aM}{b+x^2}}^{\infty}\frac{e^{-u}}{u}\,du\right]dx = \\ &= \pi I(\nu_0, T)\sqrt{aM}\int_{-\infty}^{\infty}\left[1-e^{-\frac{1}{c+y^2}}\left(1-\frac{1}{c+y^2}\right)-\left(\frac{1}{c+y^2}\right)^2\int_{\frac{1}{c+y^2}}^{\infty}\frac{e^{-u}}{u}\,du\right]dy \\ &= \pi I(\nu_k, T)\sqrt{aM}F(c)\,; \qquad y=\frac{x}{\sqrt{aM}}, \qquad c=\frac{b}{aM}, \end{aligned}\right\} \tag{8}$$

the subscript k referring to the kth line. As M increases, c decreases; and we can then write

$$F(c)=F(o)+c\dot{F}(o)+\cdots, \tag{9}$$

since $F(o)$ and $F^n(o)$ exist. It follows that

$$\pi I_k(T)=\pi\sqrt{M}I(\nu_k, T)\left(A_{ok}+\frac{A_{1k}}{M}+\cdots\right), \tag{10}$$

which shows that the emission of an individual line becomes asymptotically proportional to the square root of the emitting mass. This result was verified by Dennison[9] for the *HCl* bands and was recently confirmed by W. H. J. Childs[10] for the individual lines in the atmospheric oxygen bands. To get the total emission, we must sum (10) over all the rotational lines, obtaining

$$\pi\sum I_k(T)=\pi\sqrt{M}\sum I(\nu_k, T)\left(A_{ok}+\frac{A_{1k}}{M}+\cdots\right)\cong\pi\sqrt{M}f(T,\rho), \tag{11}$$

[9] *Phys. Rev.*, **31**, 503, 1928.

[10] *Ap. J.*, **77**, 212, 1933.

where it should be remembered that the A_{ik} are increasing functions of T and ρ.

To test equation (11), I have used F. E. Fowle's[11] data on the total absorption of water vapor in the bands 0.8 μ, ρ(0.93 μ), and Φ(1.13 μ). These are based on laboratory measurements for quantities of water vapor up to 0.6 cm of precipitable water and on results obtained in connection with the measurements of the solar constant for higher quantities of water vapor. The total absorption A, as given by his curves, is plotted against the square root of the quantity of water vapor ($\sqrt{M}$) in Figure 1. The ordinate scale of the ρ band was doubled in order to avoid overlapping with the Φ band. It is seen that, except for the end-points of the Φ band, the values follow closely the straight lines through the origin. The falling of the end-points of the Φ band below the straight line seems to be a matter of general observation. Thus, Dennison[9] in interpreting D. C. Bourgin's data on the absorption of the *HCl* lines finds that, while for tube lengths up to 0.996 cm the values computed by the square-root law are generally only slightly less than the observed values, the values computed for a tube length of 2.97 cm are considerably greater than the observed values.

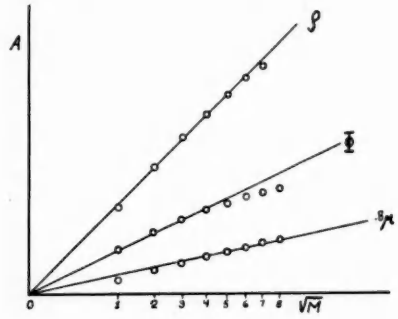

FIG. 1

This phenomenon is, in fact, to be expected on theoretical grounds. It is clear that the emission of a selectively emitting body will increase with increasing mass, until it reaches the maximum of black-body radiation. No matter how widely spaced the individual emission lines may be, there is, according to (7), a finite emission coefficient in the intervening regions, which will produce black-body emission for large masses. Equation (11) must therefore break down beyond a certain large value of M, and from there on the emission must approach black-body emission asymptotically. This is shown for a given frequency by equation (6), for with increasing β the quantity

[11] *Ibid.*, **42**, 394, 1915.

in the brackets approaches unity. When integrating in (8) over a single line, we should have made the limits of integration $-\Delta\nu$ and $+\Delta\nu$, where $\Delta\nu$ is the frequency-interval between the center of the line and the beginning of the next line. The substitution of the infinite limits is justified up to moderate values of M, because then the integrand approaches zero for large values of x. This approximation becomes serious, however, with increasing M. One therefore has to subtract from (8) the integrals from $-\infty$ to $-\Delta\nu$ and from $+\Delta\nu$ to $+\infty$. This correction was essentially carried out by R. Ladenburg and F. Reiche.[12] They find that the correction is small over a considerable region in which the asymptotic expression (10) is already valid. Beyond that region, which depends on the constants of the gas, the correction becomes important, and eventually the integral in (8) between the finite limits approaches the value of $2\Delta\nu$, which is what we should expect.

I am indebted to Professor D. H. Menzel for advice received from him during the preparation of this paper.

Massachusetts Institute of Technology and
Harvard College Observatory
January 1934

[12] *Ann. d. Phys.*, **42**, 185, 1912.

REVIEWS

Précis d'astronomie. By PAUL STROOBANT. Paris: Gauthier-Villars, 1933. Pp. vii+189. Figs. 49. Unbound, Fr. 30.

This somewhat enlarged edition of his *Précis d'astronomie pratique*, which appeared in 1904, is a résumé of the material presented by the director of the Royal Observatory of Belgium in his courses at the University of Brussels. The development of the subject since the beginning of this century has made necessary a number of additions, which are touched upon summarily.

G. V. B.

Physique moléculaire: Matière et énergie. By VICTOR HENRI. Paris: Hermann et Cie, 1933. Pp. 436. Fr. 110.

This summary of current knowledge of energy and matter as they enter into molecular processes is written from the viewpoint of the physical chemist. Beginning with an interesting historical discussion of the evidence for the discontinuity of matter, M. Henri proceeds to describe X-ray spectra and the periodic system of the elements, radioactive substances, isotopes, crystal structure, and related topics. The last two chapters are devoted to a fairly comprehensive presentation of the simpler parts of kinetic theory and of atomic structure.

The treatment throughout is compendious but precise in that the important mathematical equations involved are usually given. Naturally there is little room for derivations, but the pages are freely sprinkled with references to the original sources so that the reader is able to fill in the gaps.

P. C. K.